Thermal evolution in sedimentary basins above large shear zones and detachments

By

Alban Souche

Thesis submitted for the degree of Philosophiae Doctor

Faculty of Mathematics and Natural Sciences – Department of Geosciences

University of Oslo, Norway

August 2012

Series of dissertations submitted to the
Faculty of Mathematics and Natural Sciences, University of Oslo
No. 1254

ISSN 1501-7710

Cover: Inger Sandved Anfinsen.
Printed in Norway: AIT Oslo AS.

Produced in co-operation with Akademika publishing.
The thesis is produced by Akademika publishing merely in connection with the thesis defence. Kindly direct all inquiries regarding the thesis to the copyright holder or the unit which grants the doctorate.

Principal supervisor:

Prof. Torgeir B. Andersen

Subsidiary supervisors:

Dr. Sergei Medvedev

Dr. Marcin Dabrowski

Acknowledgements

This work would not have been accomplished without the help of many people whom I would like to thank.

I address my first acknowledgements to my supervisors Torgeir Andersen, Sergei Medvedev, and Marcin Dabrowski, for their support and their scientific guidance. I am honored to have been one of your PhD students, and I thank you for teaching me some of your singular skills. To Sergei and to Marcin, thank you for "co-supervising" this PhD, I deeply appreciated your involvement, your energy, and the trust you conferred to me throughout this project. Having three supervisors, responsible for different aspects such as the geological, mathematical and modelling components of this project, has been sometime challenging. My brain split and my focus dispersed many times, but I do feel privileged to have had the opportunity to tackle these various fields of geoscience, needed to approach the complexity of Earth's processes. In this respect, I acknowledge the opportunity that offers a cross-disciplinary research center such as PGP where mixing of sciences and knowledge brings original and rich sources of inspiration at each level of the research.

For his scientific collaboration on the project, I would like to thank Olivier Beyssac from the University Pierre et Marie Curie in Paris. Besides having provided an access to the RSMC facilities, I specially thank you for having taking part in this project and for your contribution in the elaboration of the first paper of this thesis.

As a VISTA scholar, I greatly acknowledge the Norwegian Academy of Science and Letters and Statoil for having financially supported the PhD project and provided a stimulating interaction between the academy and the industry.

Beyond sciences, my thought goes to all of you who I spent most of my time and shared my everyday's life, and who made Oslo a great place to be during the last years. Instead of starting an exhaustive list with the risk of forgetting someone, I will be brief by expressing a sincere **THANK YOU** to all of you! Thank you for having balanced my social life in proportion to the high scientific climb.

Last but not least, I want to express my deep gratitude to my family for giving me unconditional supports and encouragements over the last years.

Contents

Preface **1**

1. Introduction 1
1.1. Motivation and scope of the thesis 1
1.2. Background geology of western Norway 3
1.2.1. The Scandian continent collision 3
1.2.2. Post-Caledonian collapse and activation of the Nordfjord-Sogn Detachment Zone 3
1.2.3. The Devonian basins of western Norway 5
2. Summary of the papers 9
3. Outlook 12

***Paper I:* Thermal structure of supra-detachment basins: A case study of the Devonian basins of western Norway** **19**

1. Introduction 22
2. Geological setting 23
3. Methods 25
4. Results 26
4.1. Presence of CM 26
4.1. Temperature estimates 27
5. Discussion 29
5.1. Comparison with previous work 29
5.2. Heat from the NSDZ? 31
5.3. Regional geotherm 32
5.4. Implications 32
6. Conclusion 33

***Paper II*: Shear heating in extensional detachments: implications for the thermal history of the Devonian basins of western Norway** **39**

1. Introduction 41
2. Geological constraints of the model 44
2.1. Footwall conditions and strain partitioning in the detachment 44
2.2. The hangingwall peak temperatures 46
2.3. Model: constraints and simplifications 47
3. Model 48
3.1. Governing equations 48
3.2. Initial geotherm 49
3.3. Kinematic of the shear zone 51
3.3.1. Rheology 51
3.3.2. Constant shear strain model ($\dot{\gamma}$ -cst model) 53
3.3.3. Constant shear stress model (τ-cst model) 54
3.4. FEM strategy 55
4. Results 56
4.1. Temperature evolution and peak conditions 56
4.2. Heat produced by shear heating 56
4.3. Temperature anomaly produced by shear heating 58
5. Comparison with geological observations 59
5.1. Shear strain partitioning 59
5.2. Implications for the supra-detachment basins thermal history 60
5.3. PT-t path and retrograde overprint of rocks within the shear zone 62
6. Conclusion 63

Paper III: **Modelling thermal convection in supra-detachment basins: example from western Norway** **71**

1. Introduction 74
2. Geological setting 75
2.1. The Nordfjord-Sogn Detachment Zone 75
2.2. Formation of the Devonian supra-detachment basins 76
2.3. The basin-detachment contact 78
2.4. Evidence for fluid activity 79
3. Model setup 81
3.1. Lithospheric- and basin-scale configurations 81
3.2. Thermal and transport properties 82
3.3. Initial background temperature 85
3.4. Flow, temperature and pressure conditions (*basin model*) 86
3.5. Mathematical model for thermal convection 86
3.6. Numerical approach 87
4. Results 87
4.1. Model A: Uniform basin-fill 88
4.2. Model B: Basin layering 90
4.3. Model C: Permeability of the fault-cored pathway 91
5. Summary and discussion 93
6. Conclusion 95

Annex paper: **Influence of ice sheet and glacial erosion on passive margins of Greenland** **103**

1. Introduction 106
2. Influence of load from Greenland ice sheet 110
3. Influence of Glacial erosion: general results 111
4. Influence of ice sheet and glacial erosion: close up on Central West Greenland 115
5. Influence of glacial erosion on the evolution of Central East Greenland 117
6. Discussion 120
7. Conclusion 122

Preface

1. Introduction

1.1. Motivation and scope of the thesis

Lithospheric-scale faults and shear zones produce large offsets of crustal rock units. A number of thermal processes, such as shear heating, fluid flow, and/or metamorphic reactions, may be active during the tectonic evolution of these structures and significantly perturb the thermal state of the crust.

In compression, thrust faults may transport nappes over large distances, e.g. exceeding several hundreds of kilometres in the case of the Scandinavian Caledonides (Gee, 1978). Inverted metamorphic isograds in the Scandinavian Caledonides (Andreasson and Lagerblad, 1980) and in the Main Central Thrust of the Himalayas (England and Molnar, 1993; Pecher, 1989), amongst others, exemplify the thermal signature associated with thrusting and suggest a coupling between the tectonic setting and the thermal state of the crust. Such geological observations led to extensive research in identifying particular processes controlling the coupling and interplay between tectonics, deformation, and temperature evolution.

In extension, crustal-scale detachments may develop along low-angle normal faults and extensional shear zones (Lister et al., 1986; Wernicke, 1981, 1985, 2009). Low-angle extensional structures have been recognised in many orogenic belts such as in the Basin and Range Province (Wernicke, 1981), in the Hercynian French Massif Central (Malavieille et al., 1990; Menard and Molnar, 1988), or in the Scandinavian Caledonides in western Norway (Hossack, 1984; Norton, 1986; Seranne and Seguret, 1987). Large crustal-scale extensional detachments appear to be a common geological feature accommodating mantle exhumation both during post-orogenic extension (Davis, 1983; Lister and Davis, 1989) and during hyper-extension in rifted passive margins (Lagabrielle et al., 2010; Manatschal, 2004; Osmundsen and Ebbing, 2008).

The thermal evolution of crustal-scale detachments have been mostly determined by the study of high-grade metamorphic rocks in their footwalls (Hacker et al., 2003; Johnston et al., 2007; Jolivet et al., 1996; Labrousse et al., 2004; Root et al., 2005; Young et al., 2011). Veins analysis from detachment shear zones suggest fluid circulations during deformation but the thermal feedback to the system is still poorly quantified (Famin and Nakashima, 2005; Famin et al., 2004; Gottardi et al., 2011; Morrison and Anderson, 1998; Mulch et al., 2006). In comparison to the studies in the footwalls, the thermal evolution of the hangingwall units has received much less considerations.

The subsidence of the hangingwall of a crustal-scale detachment is usually accompanied with the formation of sedimentary basins on the top, known as supra-detachment basins (Friedmann and Burbank, 1995). The thermal characterisation of such sedimentary basins can potentially provide new insights into the thermal evolution of detachment systems. In return, a quantitative understanding of the key-processes controlling the temperature of the sediments in this particular structural setting could be profitable for potential prospectivity and exploration of resources such as hydrocarbons, ore deposits or geothermal energy. The thermal evolution of supra-detachment basins should be addressed by considering the interplay between different thermal processes operating during the dynamic evolution of the detachment.

This thesis presents an integrated cross-disciplinary study conducted to identify and quantify thermal processes operating in sedimentary basins during the development of adjacent detachment faults and shear zones. The Devonian supra-detachment basins of western Norway have been used as field analogues in the study. The selection of this geological area is motivated by the presence of a remarkable tectonic contact exposed between the Devonian basins and the crustal-scale Nordfjord-Sogn Detachment Zone, which is interpreted to be a major extensional structure active during the post-orogenic collapse of the Caledonian orogen.

Detailed field studies, sampling and laboratory analysis have been carried out in order to better characterise the thermal structure of the basins. The results of this work are presented in *Paper I*. *Paper II* and *Paper III* present two numerical studies that have been conducted to model the thermal evolution of the detachment and the adjacent sedimentary basins. In *Paper II*, we quantify the generation of shear heating produced by the development of the Nordfjord-Sogn Detachment Zone and explore its relative importance regarding the thermal structure of the Devonian basins. In *Paper III*, we analyse the potential heat transport induced by fluid flow in the system by considering thermally driven flow in the sediments. The numerical tools used in the last two studies have been developed within the framework of this PhD.

1.2. Background geology of western Norway

1.2.1. The Scandian continent collision

The Scandian continent collision is the main Caledonian mountain building event in Scandinavia and east Greenland. The collision took place after rapid plate-convergence (>10 cm/yr) between Baltica and Laurentia in the Early Silurian, which resulted in the complete closure of the Iapetus ocean at approximately 430 to 425 Ma (Torsvik and Cocks, 2005). The collision gave rise to crustal thickening and thrusting of the Caledonian nappes and a deep burial of Baltica beneath the overriding Laurentian plate (Fig. 1 a and b). In the Lower Devonian (416-400 Ma), the Caledonian mountain-belt acquired a size comparable to the present-day Himalayas (Andersen et al., 1991; Fossen, 2000, 2010; Labrousse et al., 2010; Roberts, 2003). Towards the end of the collision in the Lower Devonian, the Western Gneiss Region (WGR), which is a window of the Fennoscandian basement of Baltica, was partially subducted to reach high- and ultra-high pressure [(U)HP] metamorphic conditions at depths of ~50 to 100 km (Andersen et al., 1991; Cuthbert et al., 2000; Kylander-Clark et al., 2009; Milnes et al., 1997). The thrust-stacking and deep burial of Baltica resulted in a gravitationally unstable thick lithosphere and the onset of orogenic extension (Fig. 1c). The extensional reactivation of thrusts and the development of strike-slip and normal faults in the hinterland was contemporaneous with nappe thrusting toward the forelands (Andersen and Jamtveit, 1990; Dewey et al., 1993; Fossen, 2010; Osmundsen et al., 2005).

1.2.2. Post-Caledonian collapse and activation of the Nordfjord-Sogn Detachment Zone

The post-orogenic collapse, characterized by gravitational spreading and development of extensional detachments, resulted in the unroofing of the Caledonian orogenic root. Eclogites are exposed as lenses within the WGR, and, together with the basement gneisses, have been the focus of intense studies in recent years (Cuthbert et al., 2000; Glodny et al., 2008; Hacker et al., 2010; Hacker et al., 2003; Kylander-Clark et al., 2009; Labrousse et al., 2004; Milnes et al., 1997; Root et al., 2005). The age of the (U)HP metamorphism and the cooling history is now relatively well constrained. Here we present a brief description of the exhumation history in two main stages.

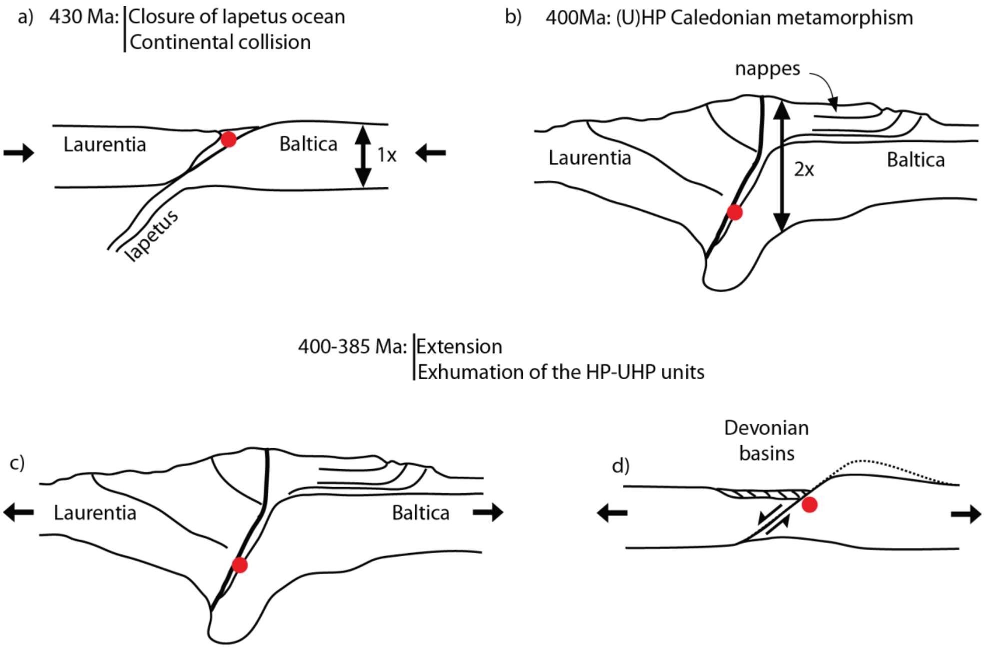

Fig. 1. Schematic cross-sections illustrating the evolution and timing of the Caledonian orogeny and collapse. The red marker illustrates the burial and exhumation of metamorphosed Caledonian nappes exposed today within the Nordfjord-Sogn Detachment Zone. a) 430 Ma: closure of the Iapetus ocean and beginning of the continent-continent collision between Baltica (Norway) and Laurentia (Greenland). b) 400 Ma: Caledonian metamorphism age of high- to ultra-high pressure (U)HP rocks and thickened orogenic crust. c-d) 400-385 Ma: decompression of the (U)HP rocks and post-orogenic extension, development of crustal-scale detachments associated with the formation of Devonian basins. Illustration based on Fossen (2000) and Hacker et al. (2010).

i) Near isothermal decompression marks the first stage of the exhumation (Labrousse et al., 2004). The fabrics associated with the initial decompression were formed at eclogite- to amphibolite-facies conditions (Engvik and Andersen, 2000; Hacker et al., 2010; Terry et al., 2000). Local partial melting is an important element in the fabric formation, particularly in the highest-grade parts of the WGR (Hacker et al., 2010; Labrousse et al., 2011). This fabric dominates in the WGR away from the detachments and records co-axial vertical shortening (e.g. Andersen et al., 1994). It formed after peak-pressure metamorphism approximately 405 Ma and gave rise to a vertical exhumation of the deepest buried rocks by 20 to 40 km (Engvik and Andersen, 2000; Fossen, 2000; Labrousse et al., 2004; Milnes et al., 1997).

ii) The second exhumation stage is associated with the development of crustal-scale detachments and sets the geodynamical framework for the development of the Devonian basins (Andersen and Jamtveit, 1990; Fossen, 2000; Fossen and Dallmeyer, 1998; Milnes et al., 1997). This stage is characterized by fast decompression and cooling of the footwall and by large-magnitude normal-shearing within the detachments. The thermo-chronology ($^{40}Ar/^{39}Ar$ mineral and model ages) of the WGR implies that the juxtaposition of low-grade metamorphic rocks in the hangingwall with high-grade metamorphic rocks of the WGR took place shortly after ~400 Ma (Andersen, 1998; Eide et al., 1999; Fossen and Dallmeyer, 1998; Fossen and Dunlap, 1998; Hacker et al., 2003; Young et al., 2011). The orogen-parallel average strike of the detachments suggests the inheritance of older collision structures and the reactivation of thrust zones (Fossen, 2000; Gabrielsen et al., 2010), however, in many localities the detachment mylonites truncate older structures such as seen in the Hornelen area (Johnston et al., 2007; Krabbendam and Dewey, 1998; Young et al., 2007; Young et al., 2011).

The Nordfjord-Sogn Detachment Zone (NSDZ) is by far the largest extensional structure formed during the post-Caledonian extension, but similar detachment systems, connected by strike-slip transfer-faults, occur further north in the Scandinavian Caledonides and also have counterparts in east Greenland (Braathen et al., 2000; Fossen, 2010; Osmundsen and Andersen, 2001). The intense top-W shearing on the NSDZ produced a several kilometre thick shear zone characterized by an average shear strain of 20 (Marques et al., 2007). The displacement along the detachment is estimated to be in the order of 60-100 km. This contributes to approximately 40-60 km of exhumation assuming an average dip of 30° along the detachment (Andersen and Jamtveit, 1990; Fossen, 2000; Hacker et al., 2003). The timing of the main crustal excision along the NSDZ is bracketed between ~405 Ma and ~395 Ma corresponding respectively to the Caledonian metamorphism and the $^{40}Ar/^{39}Ar$ cooling ages of the footwall (Andersen, 1998; Chauvet and Dallmeyer, 1992; Fossen and Dunlap, 1998; Hacker et al., 2010; Hacker et al., 2003; Young et al., 2011).

1.2.3. The Devonian basins of western Norway

The Norwegian Devonian basins (Fig. 2) differ from other "Old Red Sandstone" units deposited contemporaneously in northern Europe by their supra-detachment setting (e.g. Fossen, 2010; Osmundsen et al., 2000; Seranne and Seguret, 1987). From south to north, the Fensfjorden, Solund, Kvamshesten, Håsteinen, and Hornelen basins of western Norway are exposed in relatively narrow synclines, bounded by the NSDZ at their eastern margins, and by

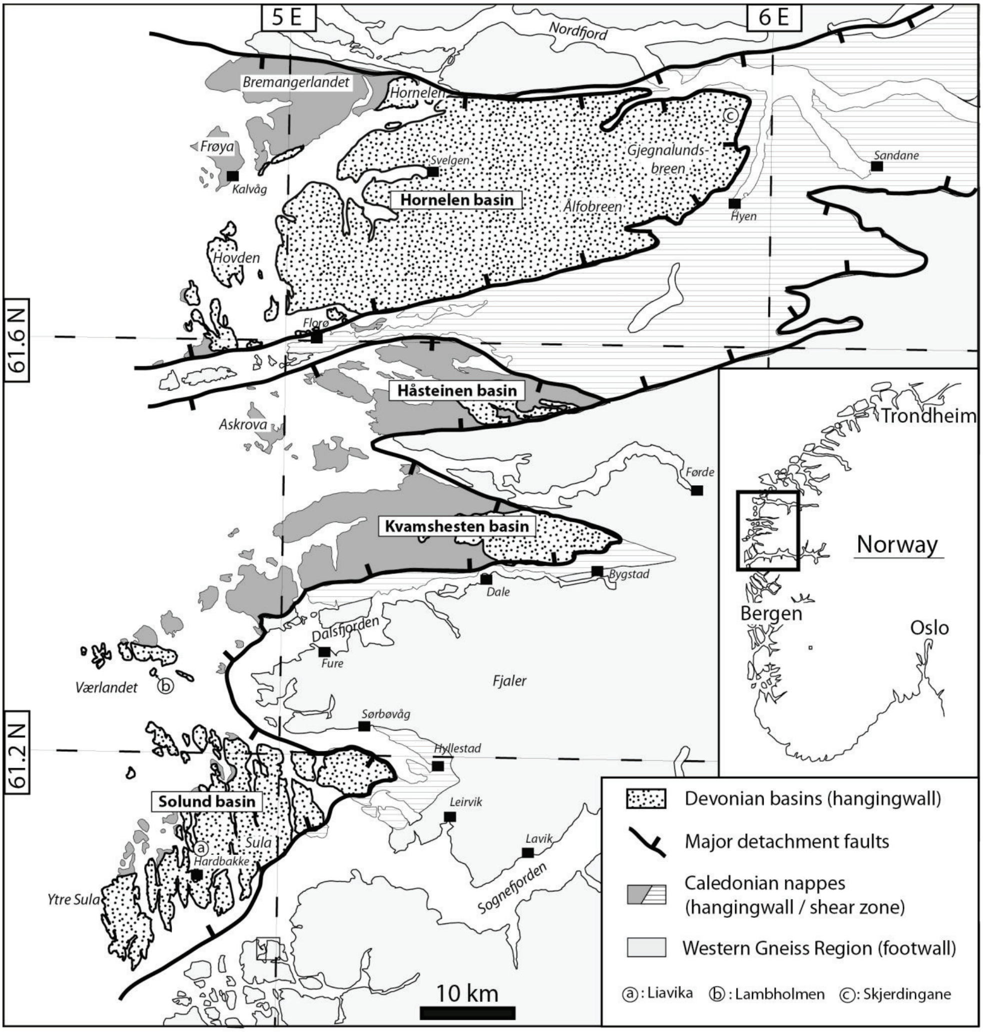

Fig. 2. Simplified geological map of western Norway showing the Nordfjord-Sogn Detachment Zone (NSDZ) with the Devonian basins juxtaposed to the Western Gneiss Region (WGR).

depositional contacts on eroded Caledonian nappes at their western margins (Fig. 2). The fish and plant fossils (Fig. 3 e and f) constrain their deposition age from Lower Devonian (416-390 Ma) for the Solund basin to Middle Devonian (390-380 Ma) for the Kvamshesten and Hornelen basins (Høegh, 1945; Kolderup, 1916). The youngest "Old Red Sandstone" basin in Norway may be Early Carboniferous as indicated by detrital mineral ages in the Asenøya basin (Eide et al., 2005). However, the earliest sedimentation is coeval with the isothermal decompression of the (U)HP rocks (405-395 Ma).

The clast provenance reflects the local origin from the eroded Caledonian nappes in the upper stratigraphic level of the hangingwall (Cuthbert, 1991; Nilsen, 1968). The immature sediment fill, particularly represented by the coarse conglomerates of the Fensfjorden, Solund and Håsteinen basins (Fig. 3 a and b) and the marginal fanglomerates of the Kvamshesten and Hornelen basins (Osmundsen and Andersen, 2001; Osmundsen et al., 1998; Osmundsen et al., 2000; Steel et al., 1977), suggests an intramontane setting with rough fault-bounded relief. The central parts of the Kvamshesten and Hornelen basins have fluvial, minor lacustrine and alluvial red sand- and siltstones (Fig. 3 c and d), whereas the Fensfjorden, Solund and the Håsteinen basins are dominated by conglomerates.

Structurally the basins were originally bounded by listric and low-angle normal faults along the detachment contact in the south and south-east margins, and by higher angle strike-slip faults in the north and north-east margins (Osmundsen and Andersen, 2001; Osmundsen et al., 1998; Osmundsen et al., 2000). The existence of listric faults is indirectly deduced from the internal basin architecture characterized by nearly uniform eastward titling of the layering (25-30°E in Hornelen) and interpreted as rollover deformations above the faults (Osmundsen et al., 1998). As describe by several studies (Osmundsen et al., 2000; Seguret et al., 1989; Steel et al., 1977) the lateral growth, and the great stratigraphic thickness of the basins (>25 km in the Hornelen basin) is explained by eastward shift of the depo-centers during the extension.

In contrast to a large number of detailed sedimentological and tectono-stratigraphic studies, the thermal states of the basins have been studied only scarcely. Palaeomagnetic data suggest a thermo-chemical resetting of the remanent magnetism after deposition (Smethurst, 1990; Torsvik et al., 1988). Braathen et al. (2004) described a complex structure (including sheared conglomerates in a phyllonitic matrix) at the base of the Kvamshesten basin along the contact with the NSDZ. Low greenschist facies metamorphism accompanied by localized ductile deformation of conglomerates along the NSDZ was also reported in the Solund basin (Seranne and Seguret, 1987). The mineralogy of authigenic minerals and fluid inclusion analysis of metamorphic veins found in the Hornelen, Kvamshesten and Solund basins document an incipient regional Devonian metamorphism (Svensen et al., 2001). These authors also suggest that the temperature and burial depth of the basins increased southward from 250 ± 20 °C at a depth of 9.1 ± 1.6 km in the Hornelen and Kvamshesten basins to 315 ± 15 °C at a depth of 13.4 ± 0.6 km in the Solund basin.

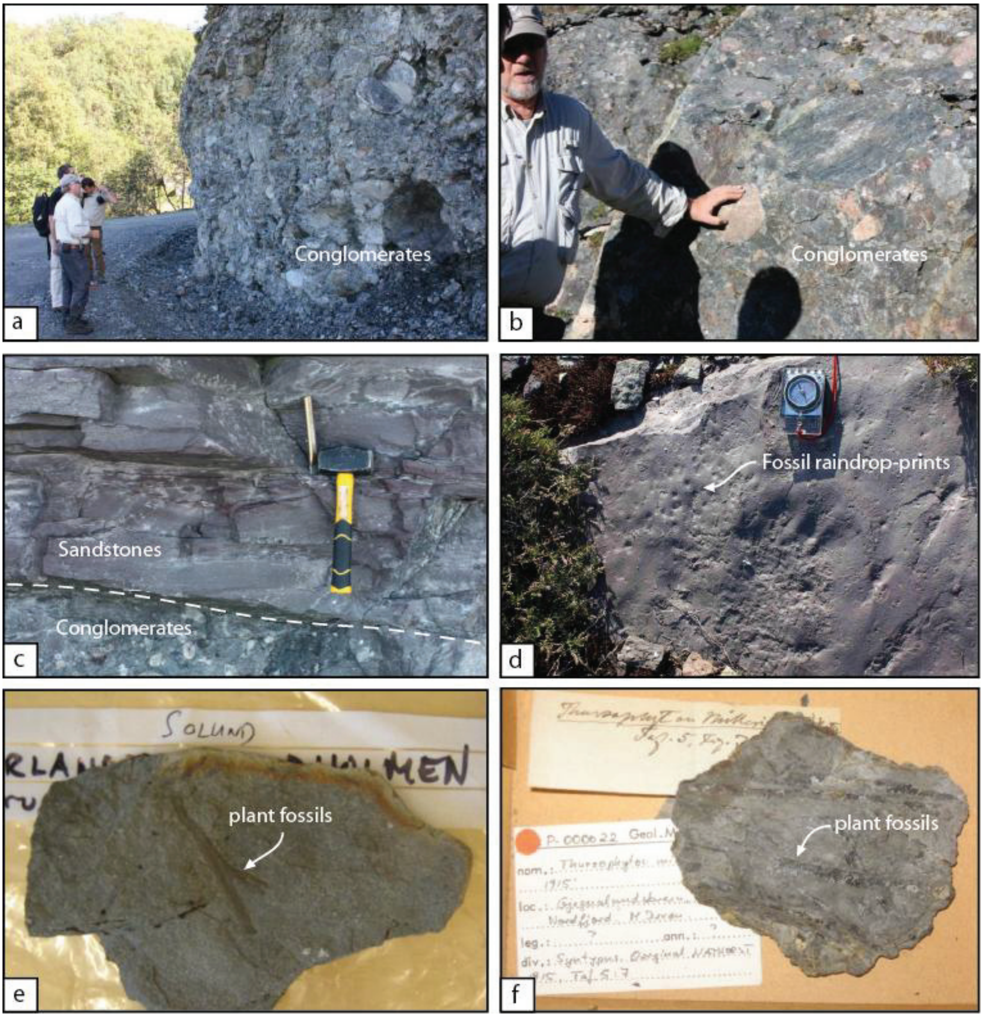

Fig. 3. Some examples of rocks and fossil plants found in the Devonian basins of western Norway. a-b) Coarse conglomerates in the Solund basin. c) Red sandstones and conglomerates in the Solund basin, near Liavika. d) Surface of a siltstone layer with presence of fossil raindrop-prints in the Solund basin, near Liavika. e-f) Devonian plant fossils in siltstones from the Solund basin, at Lambholmen, and from the easternmost parts of the Hornelen basin, near Skjerdingane, respectively.

2. Summary of the papers

This thesis is a collection of three main papers that first present field and laboratory-based geological data (*Paper I*) that are later used and discussed in numerical studies (*Paper II* and *Paper III*). *Paper I* is published in the *Journal of Geological Society of London*, *Paper II* is submitted to *Tectonophysics* and *Paper III* is prepared for submission to *Geofluids*.

In *annex*, the thesis contains a fourth paper, which presents the results of a side project started before but carried out mainly during the period of the PhD. This paper discusses the origin of uplifts along Greenland's margins and is submitted to *Geomorphology*.

Paper I: *Thermal structure of supra-detachment basins, a case study of the Devonian basins of western Norway*

This paper presents new peak temperature estimates from the three main Devonian basins of western Norway and explores the thermal structure of the basins in relation to the distance to the detachment contact. These data were obtained using Raman spectroscopy on detrital carbonaceous material found in the sediments. Extensive field work and systematic sampling and analysis of the rocks throughout the stratigraphy of the Hornelen, Kvamshesten and Solund basins, have been carry out, but the presence of the required carbonaceous material was only preserved in some rare plant fossil-bearing siltstones. The data set presented in this paper was combined with previous fluid inclusion data and peak temperature estimates from metamorphic veins found in the same basins (Svensen et al., 2001). A lateral variation of the peak temperature conditions, elevated towards the contact with the shear zone of the Nordfjord-Sogn Detachment, is demonstrated. Two main conclusions are drawn in this paper; first that the development of the detachment controlled the peak temperature distribution in the supra-detachment basins, and secondly, that sediments close to the detachment contact may have been exposed to temperature up to 100 ^{o}C higher than few kilometers away from the detachment. The temperature estimates presented in this paper are used to discuss the model results obtained in *Paper II* and *Paper III*.

<u>Paper II</u>: Shear heating in extensional detachments: implications for the thermal history of the Devonian basins of western Norway

This paper presents a numerical study conducted to quantify the influence of shear heating generated by rock deformation during the development of the Nordfjord-Sogn Detachment Zone. The model geometry and a number of important model constraints are based on published geological observations and data. Shear heating is estimated with a lower and upper bound depending on two kinematic models used to estimate the velocity in the shear zone of the detachment. The model results illustrate the importance of shear heating as a heat source in tectonic settings characterized by the excision of a major portion of the crust along a main shear zone. The results are compared with geological data from the Devonian basins and from exhumed Caledonian nappes exposed in the footwall of the detachment. We conclude that shear heating may lead to an increase of the peak temperature conditions in the order of 100 °C close to the detachment contact and contribute up to 25% of the thermal budget of the supra-detachment basins.

<u>Paper III</u>: Modelling thermal convection in supra-detachment basins: example from western Norway

In this paper, we quantify the importance of thermally driven fluid flow as a heat transport mechanism in supra-detachment basins shortly after the exhumation of warmer footwalls. The flow is computed from a regional background temperature field obtained from the study presented in *Paper II*. Geological features observed in the Devonian basins of western Norway, such as the internal sedimentary layering or the contact with the detachment fault, are presented and their potential impact on the fluid circulation in the basins is analyzed and discussed. Different models are tested with homogeneous and layered basin-fill and with material transport properties corresponding to siltstones and sandstones. Thermally driven fluid flow is expected in supra-detachment setting as a transient process shortly after the exhumation of warmer footwalls and before the thermal relaxation of the isotherms in the area. The fluid flow may significantly affect the temperature distribution in the upper five kilometres of the basin where the rock permeability allows fluid circulation. The temperature anomaly induced by the flow may locally reach 80 °C. The presence of fluid pathways along the detachment contact has an important impact on the flow and allows an efficient drainage of the basin by channelizing fluids upward along the detachment.

Annex paper: Influence of ice sheet and glacial erosion on passive margins of Greenland

This paper discusses the origin of the uplift of Mesozoic and Cenozoic marine sediments along Greenland's margins by quantifying isostatic uplift caused by ice carving of the fjord systems. Combining digital elevation models and ice thickness data available from Greenland, the model estimates the amount of material eroded away from the fjords and balances the corresponding mass load onto an elastic plate model. Resulting vertical motions are estimated for the entire Greenland area. This work is a generalization of the previous study conducted in the Scoresby Sund fjord region by Medvedev et al. (2008). The numerical model developed in this study could be applied to other part of the world where erosion may locally incise the landscape. Western Norway, the main subject of the thesis, presents similar fjord system and was considered as potential study area.

3. Outlook

During this PhD study, two distinct thermal solvers have been developed in order to quantify shear heating from active shear zones and thermally driven fluid flow in permeable aquifers. The models were applied to understand the thermal evolution of supra-detachment basins with a particular focus on the Devonian basins of western Norway. The methods and results, however, can be extended to other basins that present similar geological features such as basal shear zones and detachments. In the following, we give an example of possible future investigations where similar thermal processes as assessed in this study could play a role.

Low-angle detachments associated with the formation of deep supra-detachment basins have been interpreted from geophysical surveys in several areas along the Mid-Norwegian shelf (Lundin and Doré, 1997; Osmundsen et al., 2005; Ren et al., 1998). These structures and accompanying basins have been the topic of several projects dealing with the details of the extensional geometries, the determination of the stretching, the link to magmatism, as well as thermo-kinematic modelling (Gernigon et al., 2006; Gernigon et al., 2004; Gernigon et al., 2003). Upper Cretaceous fault complexes are well-imaged on seismic data in the outer Vøring Basin (Fig. 4), including the North and South Gjallar ridges and the Rån Ridge. These ridges are currently being explored by the petroleum industry and few wells have been drilled. The Gjallar well (6704/12-1) drilled in 1999 revealed a high temperature gradient (52 °C/km). Improved constraints on the thermal history of these basins may lead to reduced future exploration risks.

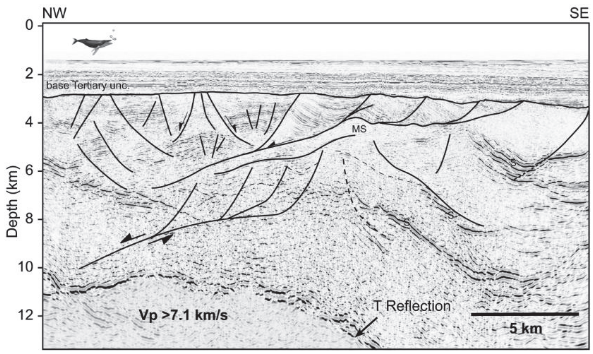

Fig. 4. Structural style of the North Gjallar Ridge on the outer Vøring Basin. Rollover deformation structures in sedimentary basins are observed above detachments in mobile shales (MS). Figure from Gernigon et al. (2003).

References

Andersen, T. B., 1998, Extensional tectonics in the Caledonides of southern Norway, an overview: Tectonophysics, v. 285, no. 3-4, p. 333-351.

Andersen, T. B., and Jamtveit, B., 1990, Uplift of deep crust during orogenic extensional collapse: A model based on field studies in the Sogn-Sunnfjord Region of western Norway: Tectonics, v. 9, no. 5, p. 1097-1111.

Andersen, T. B., Jamtveit, B., Dewey, J. F., and Swensson, E., 1991, Subduction and eduction of continental crust: major mechanisms during continent-continent collision and orogenic extensional collapse, a model based on the south Norwegian Caledonides: Terra Nova, v. 3, no. 3, p. 303-310.

Andersen, T. B., Osmundsen, P. T., and Jolivet, L., 1994, Deep crustal fabrics and a model for the extensional collapse of the southwest Norwegian Caledonides: Journal of Structural Geology, v. 16, no. 9, p. 1191-1203.

Andreasson, P. G., and Lagerblad, B., 1980, Occurrence and significance of inverted metamorphic gradients in the western Scandinavian Caledonides: Journal of the Geological Society, v. 137, no. 3, p. 219-230.

Braathen, A., Nordgulen, Ø., Osmundsen, P.-T., Andersen, T. B., Solli, A., and Roberts, D., 2000, Devonian, orogen-parallel, opposed extension in the Central Norwegian Caledonides: Geology, v. 28, no. 7, p. 615-618.

Braathen, A., Osmundsen, P. T., and Gabrielsen, R. H., 2004, Dynamic development of fault rocks in a crustal-scale detachment: An example from western Norway: Tectonics, v. 23, no. 4, p. TC4010.

Chauvet, A., and Dallmeyer, R. D., 1992, 40Ar/39Ar mineral dates related to Devonian extension in the southwestern Scandinavian Caledonides: Tectonophysics, v. 210, no. 1-2, p. 155-177.

Cuthbert, S. J., 1991, Evolution of the Devonian Hornelen Basin, west Norway: new constraints from petrological studies of metamorphic clasts: Developments in sedimentary provenance studies, p. 343-360.

Cuthbert, S. J., Carswell, D. A., Krogh-Ravna, E. J., and Wain, A., 2000, Eclogites and eclogites in the Western Gneiss region, Norwegian Caledonides: Lithos, v. 52, no. 1-4, p. 165-195.

Davis, G. H., 1983, Shear-zone model for the origin of metamorphic core complexes: Geology, v. 11, no. 6, p. 342-347.

Dewey, J. F., Ryan, P. D., and Andersen, T. B., 1993, Orogenic uplift and collapse, crustal thickness, fabrics and metamorphic phase changes: the role of eclogites: Geological Society, London, Special Publications, v. 76, no. 1, p. 325-343.

Eide, E. A., Haabesland, N. E., Osmundsen, P. T., Andersen, T. B., Roberts, D., and Kendrick, M. A., 2005, Modern techniques and Old Red problems - Determining the age of continental sedimentary deposits with ^{40}Ar/ ^{39}Ar provenance analysis in west-central Norway: Norsk Geologisk Tidsskrift, v. 85, no. 1-2, p. 133-145.

Eide, E. A., Torsvik, T. H., Andersen, T. B., and Arnaud, N. O., 1999, Early Carboniferous Unroofing in Western Norway: A Tale of Alkali Feldspar Thermochronology: The Journal of Geology, v. 107, no. 3, p. 353-374.

England, P., and Molnar, P., 1993, The interpretation of inverted metamorphic isograds using simple physical calculations: Tectonics, v. 12, no. 1, p. 145-157.

Engvik, A. K., and Andersen, T. B., 2000, Evolution of Caledonian deformation fabrics under eclogite and amphibolite facies at Vardalsneset, Western Gneiss Region, Norway: Journal of Metamorphic Geology, v. 18, no. 3, p. 241-257.

Famin, V., and Nakashima, S., 2005, Hydrothermal fluid venting along a seismogenic detachment fault in the Moresby rift (Woodlark basin, Papua New Guinea): Geochem. Geophys. Geosyst., v. 6, no. 12, p. Q12003.

Famin, V., Philippot, P., Jolivet, L., and Agard, P., 2004, Evolution of hydrothermal regime along a crustal shear zone, Tinos Island, Greece: Tectonics, v. 23, no. 5, p. TC5004.

Fossen, H., 2000, Extensional tectonics in the Caledonides: Synorogenic or postorogenic: Tectonics, v. 19, no. 2, p. 213-224.

-, 2010, Extensional tectonics in the North Atlantic Caledonides: A regional view, p. 767-793.

Fossen, H., and Dallmeyer, R. D., 1998, $^{40}Ar/^{39}Ar$ muscovite dates from the nappe region of southwestern Norway: dating extensional deformation in the Scandinavian Caledonides: Tectonophysics, v. 285, no. 1–2, p. 119-133.

Fossen, H., and Dunlap, W. J., 1998, Timing and kinematics of Caledonian thrusting and extensional collapse, southern Norway: evidence from 40Ar/39Ar thermochronology: Journal of Structural Geology, v. 20, no. 6, p. 765-781.

Friedmann, S. J., and Burbank, D. W., 1995, Rift basins and supradetachment basins: Intracontinental extensional end-members: Basin Research, v. 7, no. 2, p. 109-127.

Gabrielsen, R. H., Faleide, J. I., Pascal, C., Braathen, A., Nystuen, J. P., Etzelmuller, B., and O'Donnell, S., 2010, Latest Caledonian to Present tectonomorphological development of southern Norway: Marine and Petroleum Geology, v. 27, no. 3, p. 709-723.

Gee, D. G., 1978, Nappe displacement in the Scandinavian Caledonides: Tectonophysics, v. 47, no. 3–4, p. 393-419.

Gernigon, L., Lucazeau, F., Brigaud, F., Ringenbach, J.-C., Planke, S., and Le Gall, B., 2006, A moderate melting model for the Vøring margin (Norway) based on structural observations and a thermo-kinematical modelling: Implication for the meaning of the lower crustal bodies: Tectonophysics, v. 412, no. 3–4, p. 255-278.

Gernigon, L., Ringenbach, J.-C., Planke, S., and Le Gall, B., 2004, Deep structures and breakup along volcanic rifted margins: insights from integrated studies along the outer Vøring Basin (Norway): Marine and Petroleum Geology, v. 21, no. 3, p. 363-372.

Gernigon, L., Ringenbach, J. C., Planke, S., Le Gall, B., and Jonquet-Kolstø, H., 2003, Extension, crustal structure and magmatism at the outer Vøring Basin, Norwegian margin: Journal of the Geological Society, v. 160, no. 2, p. 197-208.

Glodny, J., Kühn, A., and Austrheim, H., 2008, Diffusion versus recrystallization processes in Rb-Sr geochronology: Isotopic relics in eclogite facies rocks, Western Gneiss Region, Norway: Geochimica et Cosmochimica Acta, v. 72, no. 2, p. 506-525.

Gottardi, R., Teyssier, C., Mulch, A., Vennemann, T. W., and Wells, M. L., 2011, Preservation of an extreme transient geotherm in the Raft River detachment shear zone: Geology, v. 39, no. 8, p. 759-762.

Hacker, B. R., Andersen, T. B., Johnston, S., Kylander-Clark, A. R. C., Peterman, E. M., Walsh, E. O., and Young, D., 2010, High-temperature deformation during continental-margin subduction & exhumation: The ultrahigh-pressure Western Gneiss Region of Norway: Tectonophysics, v. 480, no. 1–4, p. 149-171.

Hacker, B. R., Andersen, T. B., Root, D. B., Mehl, L., Mattinson, J. M., and Wooden, J. L., 2003, Exhumation of high-pressure rocks beneath the Solund Basin, Western Gneiss Region of Norway: Journal of Metamorphic Geology, v. 21, no. 6, p. 613-629.

Hossack, J. R., 1984, The geometry of listric growth faults in the Devonian basins of Sunnfjord, W Norway: Journal of the Geological Society, v. 141, no. 4, p. 629-637.

Høegh, O. A., 1945, Contributions to the Devonian flora of western Norway III.: Norsk Geologisk Tidsskrift, v. 25, p. 183-192.

Johnston, S., Hacker, B. R., and Ducea, M. N., 2007, Exhumation of ultrahigh-pressure rocks beneath the Hornelen segment of the Nordfjord-Sogn Detachment Zone, western Norway: Geological Society of America Bulletin, v. 119, no. 9-10, p. 1232-1248.

Jolivet, L., Goffé, B., Monié, P., Truffert-Luxey, C., Patriat, M., and Bonneau, M., 1996, Miocene detachment in Crete and exhumation P-T-t paths of high-pressure metamorphic rocks: Tectonics, v. 15, no. 6, p. 1129-1153.

Kolderup, C. F., 1916, Bulandets og Værlandets konglomerat og sandstensfelt.: Bergens Museums Aarbok 1915-16, v. Naturvidenskabelig Række, no. 8, p. 26.

Krabbendam, M., and Dewey, J. F., 1998, Exhumation of UHP rocks by transtension in the Western Gneiss Region, Scandinavian Caledonides: Geological Society, London, Special Publications, v. 135, no. 1, p. 159-181.

Kylander-Clark, A. R. C., Hacker, B. R., Johnson, C. M., Beard, B. L., and Mahlen, N. J., 2009, Slow subduction of a thick ultrahigh-pressure terrane: Tectonics, v. 28, no. 2, p. TC2003.

Labrousse, L., Hetényi, G., Raimbourg, H., Jolivet, L., and Andersen, T. B., 2010, Initiation of crustal-scale thrusts triggered by metamorphic reactions at depth: Insights from a comparison between the Himalayas and Scandinavian Caledonides: Tectonics, v. 29, no. 5.

Labrousse, L., Jolivet, L., Andersen, T. B., Agard, P., Hébert, R., Maluski, H., and Schärer, U., 2004, Pressure-temperature-time deformation history of the exhumation of ultra-high pressure rocks in the Western Gneiss Region, Norway: Geological Society of America Special Papers, v. 380, p. 155-183.

Labrousse, L., Prouteau, G., and Ganzhorn, A. C., 2011, Continental exhumation triggered by partial melting at ultrahigh pressure: Geology, v. 39, no. 12, p. 1171-1174.

Lagabrielle, Y., Labaume, P., and de Saint Blanquat, M., 2010, Mantle exhumation, crustal denudation, and gravity tectonics during Cretaceous rifting in the Pyrenean realm (SW Europe): Insights from the geological setting of the lherzolite bodies: Tectonics, v. 29, no. 4, p. TC4012.

Lister, G. S., and Davis, G. A., 1989, The origin of metamorphic core complexes and detachment faults formed during Tertiary continental extension in the northern Colorado River region, U.S.A: Journal of Structural Geology, v. 11, no. 1–2, p. 65-94.

Lister, G. S., Etheridge, M. A., and Symonds, P. A., 1986, Detachment faulting and the evolution of passive continental margins: Geology, v. 14, no. 3, p. 246-250.

Lundin, E. R., and Doré, A. G., 1997, A tectonic model for the Norwegian passive margin with implications for the NE Atlantic: Early Cretaceous to break-up: Journal of the Geological Society, v. 154, no. 3, p. 545-550.

Malavieille, J., Guihot, P., Costa, S., Lardeaux, J. M., and Gardien, V., 1990, Collapse of the thickened Variscan crust in the French Massif Central: Mont Pilat extensional shear zone and St. Etienne Late Carboniferous basin: Tectonophysics, v. 177, no. 1–3, p. 139-149.

Manatschal, G., 2004, New models for evolution of magma-poor rifted margins based on a review of data and concepts from West Iberia and the Alps: International Journal of Earth Sciences, v. 93, no. 3, p. 432-466.

Marques, F. O., Schmid, D. W., and Andersen, T. B., 2007, Applications of inclusion behaviour models to a major shear zone system: The Nordfjord-Sogn Detachment Zone in western Norway: Journal of Structural Geology, v. 29, no. 10, p. 1622-1631.

Medvedev, S., Hartz, E. H., and Podladchikov, Y. Y., 2008, Vertical motions of the fjord regions of central East Greenland: Impact of glacial erosion, deposition, and isostasy: Geology, v. 36, no. 7, p. 539-542.

Menard, G., and Molnar, P., 1988, Collapse of a Hercynian Tibetan Plateau into a late Palaeozoic European Basin and Range province: Nature, v. 334, no. 6179, p. 235-237.

Milnes, A. G., Wennberg, O. P., Skår, Ø., and Koestler, A. G., 1997, Contraction, extension and timing in the South Norwegian Caledonides: the Sognefjord transect, Volume 121, p. 123-148.

Morrison, J., and Anderson, J. L., 1998, Footwall Refrigeration Along a Detachment Fault: Implications for the Thermal Evolution of Core Complexes: Science, v. 279, no. 5347, p. 63-66.

Mulch, A., Teyssier, C., Cosca, M. A., and Vennemann, T. W., 2006, Thermomechanical analysis of strain localization in a ductile detachment zone: Journal of Geophysical Research B: Solid Earth, v. 111, no. 12.

Nilsen, T. H., 1968, The relationship of sedimentation to tectonics in the Solund Devonian district of southwestern Norway.: Nor. Geol. Unders. Bull., no. 292, p. 1-20.

Norton, M. G., 1986, Late Caledonide Extension in western Norway: A response to extreme crustal thickening: Tectonics, v. 5, no. 2, p. 195-204.

Osmundsen, P. T., and Andersen, T. B., 2001, The middle Devonian basins of western Norway: Sedimentary response to large-scale transtensional tectonics?: Tectonophysics, v. 332, no. 1-2, p. 51-68.

Osmundsen, P. T., Andersen, T. B., Markussen, S., and Svendby, A. K., 1998, Tectonics and sedimentation in the hangingwall of a major extensional detachment: The Devonian Kvamshesten Basin, western Norway: Basin Research, v. 10, no. 2, p. 213-234.

Osmundsen, P. T., Bakke, B., Svendby, A. K., and Andersen, T. B., 2000, Architecture of the middle Devonian Kvamshesten group, Western Norway: Sedementary response to deformation above a ramp-flat extensional fault, p. 503-535.

Osmundsen, P. T., Braathen, A., Sommaruga, A., Skilbrei, J. R., Nordgulen, Ø., Roberts, D., Andersen, T. B., Olesen, O., and Mosar, J., 2005, Metamorphic core complexes and gneiss-cored culminations along the Mid-Norwegian margin: an overview and some current ideas, *in* Bjørn T.G Wandås, J. P. N. E. E., and Felix, G., eds., Norwegian Petroleum Society Special Publications, Volume Volume 12, Elsevier, p. 29-41.

Osmundsen, P. T., and Ebbing, J., 2008, Styles of extension offshore mid-Norway and implications for mechanisms of crustal thinning at passive margins: Tectonics, v. 27, no. 6.

Pecher, A., 1989, The metamorphism in the Central Himalaya: Journal of Metamorphic Geology, v. 7, no. 1, p. 31-41.

Ren, S., Skogseid, J., and Eldholm, O., 1998, Late Cretaceous-Paleocene extension on the Vøring Volcanic Margin: Marine Geophysical Research, v. 20, no. 4, p. 343-369.

Roberts, D., 2003, The Scandinavian Caledonides: event chronology, palaeogeographic settings and likely modern analogues: Tectonophysics, v. 365, no. 1–4, p. 283-299.

Root, D. B., Hacker, B. R., Gans, P. B., Ducea, M. N., Eide, E. A., and Mosenfelder, J. L., 2005, Discrete ultrahigh-pressure domains in the Western Gneiss Region, Norway: implications for formation and exhumation: Journal of Metamorphic Geology, v. 23, no. 1, p. 45-61.

Seguret, M., Seranne, M., Chauvet, A., and Brunel, M., 1989, Collapse basin: a new type of extensional sedimentary basin from the Devonian of Norway: Geology, v. 17, no. 2, p. 127-130.

Seranne, M., and Seguret, M., 1987, The Devonian basins of western Norway: tectonics and kinematics of an extending crust: Continental extensional tectonics, p. 537-548.

Smethurst, M. A., 1990, Palaeomagnetism of the Kvamshesten and Hornelen Old Red Sandstone Basins, western Norway: Geophysical Journal International, v. 102, no. 3, p. 585-601.

Steel, R. J., Mæhle, S., Nilsen, H., Røe, S. L., and Spinnanger, A., 1977, Coarsening-upward cycles in the alluvium of Hornelen Basin (Devonian) Norway: Sedimentary response to tectonic events: Geological Society of America Bulletin, v. 88, no. 8, p. 1124-1134.

Svensen, H., Jamtveit, B., Banks, D. A., and Karlsen, D., 2001, Fluids and halogens at the diagenetic–metamorphic boundary: evidence from veins in continental basins, western Norway: Geofluids, v. 1, no. 1, p. 53-70.

Terry, M. P., Robinson, P., and Krogh Ravna, E. J., 2000, Kyanite eclogite thermobarometry and evidence for thrusting of UHP over HP metamorphic rocks, Nordoyane, Western Gneiss Region, Norway: American Mineralogist, v. 85, no. 11-12, p. 1637-1650.

Torsvik, T. H., and Cocks, L. R. M., 2005, Norway in space and time: A Centennial cavalcade: Norsk Geologisk Tidsskrift, v. 85, no. 1-2, p. 73-86.

Torsvik, T. H., Sturt, B. A., Ramsay, D. M., Bering, D., and Fluge, P. R., 1988, Palaeomagnetism, magnetic fabrics and the structural style of the Hornelen Old Red Sandstone, western Norway: Journal - Geological Society (London), v. 145, no. 3, p. 413-430.

Wernicke, B., 1981, Low-angle normal faults in the Basin and Range Province: nappe tectonics in an extending orogen: Nature, v. 291, no. 5817, p. 645-648.

-, 1985, Uniform-sense normal simple shear of the continental lithosphere: Canadian Journal of Earth Sciences, v. 22, no. 1, p. 108-125.

-, 2009, The detachment era (1977-1982) and its role in revolutionizing continental tectonics, p. 1-8.

Young, D. J., Hacker, B. R., Andersen, T. B., and Corfu, F., 2007, Prograde amphibolite facies to ultrahigh-pressure transition along Nordfjord, western Norway: Implications for exhumation tectonics: Tectonics, v. 26, no. 1, p. TC1007.

Young, D. J., Hacker, B. R., Andersen, T. B., and Gans, P. B., 2011, Structure and 40Ar/39Ar thermochronology of an ultrahigh-pressure transition in western Norway: Journal of the Geological Society, v. 168, no. 4, p. 887-898.

Paper I: Thermal structure of supra-detachment basins: A case study of the Devonian basins of western Norway

Published in the *Journal of the Geological Society, London*, Vol. **169**, 2012, pp. 427–434.
doi: 10.1144/0016-76492011-155

Thermal structure of supra-detachment basins: A case study of the Devonian basins of western Norway.

Alban Souche[1], Olivier Beyssac[2], Torgeir B. Andersen[1]

[1]Physics of Geological Processes (PGP), University of Oslo, P.O. Box 1048, Blindern, 0316 Oslo, Norway

[2]Institut de Minéralogie et de Physique des Milieux Condensés (IMPMC), CNRS-UPMC, Case Courrier 115, 4 place Jussieu, 75005 Paris, France

Abstract:

We investigate the peak temperatures of the Devonian Hornelen, Kvamshesten and Solund basins in SW Norway in order to constrain their thermal history. These basins are the three largest Devonian units exposed in Norway and were formed as supra-detachment basins in the hangingwall of the Nordfjord Sogn Detachment Zone (NSDZ). The peak temperatures of the basins were obtained using a geothermometer based on Raman spectroscopy of carbonaceous material (RSCM) on detrital carbonaceous plant fossils. The data confirm an anchizone to low greenschist facies metamorphism with temperatures (± 30 ^{o}C) of 284 ^{o}C to 301 ^{o}C in the Hornelen and Solund basins and a significantly higher, 345 ^{o}C in the Kvamshesten basin. The temperature increases toward the detachment fault and cannot be explained by ordinary burial alone. In the Kvamshesten basin this temperature increase is close to 100 ^{o}C. The new data demonstrate that exhumation of high-grade rocks in the footwall in the NSDZ played an important role in controlling temperatures in the hangingwall. We conclude that the dynamic evolution along large-scale detachments may introduce heat at the base of the hangingwall and thereby control the thermal state of supra-detachment basins formed during extension.

1. Introduction

Crustal extensional detachments are remarkable geological features that may produce vast metamorphic discontinuities between the hangingwall and the footwall rocks across high-strain shear zones. Since the 1980-ies, low-angle normal faults have provided important conceptual and quantitative models of the dynamics and evolution of large-magnitude crustal extension (e.g. Wernicke 1985, 2009; Lister *et al.* 1986; Jolivet *et al.* 2010), but important questions remain regarding the thermal evolution of such systems. The classical approach to estimate geotherms above a uniformly stretched lithosphere (i.e. McKenzie 1978) cannot be employed in detachment areas that are characterised by strong localised deformation along shear zones with asymmetric geometries. Common features of metamorphic core complexes in detachment footwalls are rapid exhumation accompanied by quasi-isothermal decompressions (Jolivet *et al.* 1996; Labrousse *et al.* 2004). At these conditions, the thermal evolution of the system is likely to be influenced by a temperature contrast between the "hot" footwall and the "cold" hangingwall. Depending on the exhumation rate of the footwall and the sedimentation rate in the hangingwall, this asymmetry would affect the regional geotherms in the supra-detachment basins and their thermal history during burial. Recent studies have reported large variations in temperature across detachment shear zone toward deeper parts of the footwall (Mulch *et al.* 2006 ; Cottle *et al.* 2011; Gottardi *et al.* 2011). However, such temperature gradient in a hangingwall, and more specifically within supra-detachment basins, has not yet been documented.

A well-known example of post-orogenic extension producing a very large detachment is exposed in western Norway. The Nordfjord Sogn Detachment Zone (NSDZ) juxtaposes low-grade Caledonian nappes in the hangingwall against high-grade eclogite facies rocks across a several kilometres thick mylonite zone (Andersen & Jamtveit 1990; Norton 1987; Osmundsen *et al.* 2000) (Fig. 1). The direct contact between the supra-detachment basins and the detachment mylonites provides an excellent study area to investigate the thermal state of the basins as a function of the distance to the detachment. In this study, we used a geothermometer based on Raman Spectroscopy of Carbonaceous Material (RSCM thermometry – Beyssac *et al.* 2002) and its extension to low-temperature (Lahfid *et al.* 2010).

2. Geological setting

The Norwegian Devonian basins differ from other "Old Red" sediments deposited contemporaneously in northern Europe by their supra-detachment setting (i.e. Fossen 2010, Osmundsen *et al.* 2000; Seranne & Seguret 1987). They are located at the top of the hangingwall of the large-scale extensional NSDZ and other extensional shear zones near Røragen and along the Møre-Trøndelag Fault Complex (McClay *et al.* 1986; Osmundsen *et al.* 2005). The detachments were initiated by the late- to post-orogenic extensional collapse in the Early Devonian, and the formation and filling of the basins were coeval with the main movement on the detachments (i.e. Fossen 2000; Norton 1987; Seranne *et al.* 1989; Seranne & Seguret 1987). The Hornelen, Kvamshesten, and Solund basins (north to south) of western Norway are preserved in synclines, bounded to the east by the NSDZ, and by depositional unconformities on the eroded Caledonian nappes in the west and north-west (Fig. 1). Sporadically preserved plant and fish fossils constrain their deposition from the Early Devonian (416 - 391 Ma) for the Solund basin to Middle Devonian (391-372 Ma) for the Kvamshesten and Hornelen basins respectively (Høegh 1945; Kolderup 1916, 1921, 1927).

In contrast to a large number of detailed sedimentological and tectono-stratigraphic studies (Osmundsen & Andersen 2001; Osmundsen *et al.* 1998, 2000; Steel *et al.* 1977), the thermal states of the basins have only been provisionally studied. Palaeomagnetic data suggest a thermo-chemical resetting of the remanent magnetism after deposition (e.g. Smethurst 1990; Torsvik *et al.* 1988). It has also been shown that minor reactivation of the NSDZ partially reset the palaeomagnetic remanence of breccias along the detachment in the Permian and locally in the Late Jurassic/Early Cretaceous (Eide *et al.* 1997; Torsvik *et al.* 1992). Braathen *et al.* (2004) described a complex structure including conglomerates with deformed pebbles in a phyllonitic matrix at the base of the hangingwall of the NSDZ underneath the Kvamshesten basin. Lower greenschist facies metamorphism accompanied by localised ductile deformation of conglomerates along the detachment was also reported from the Solund basin (Seranne & Seguret 1987). This basin has been interpreted to be the most deeply buried Devonian basin of western Norway.

In addition, the mineralogy of authigenic minerals and fluid inclusion analysis of metamorphic veins found throughout the Hornelen, Kvamshesten and Solund basins document the incipient regional Devonian metamorphism (Svensen *et al.* 2001). These authors also suggest that the temperature and burial of the basins increases southward from

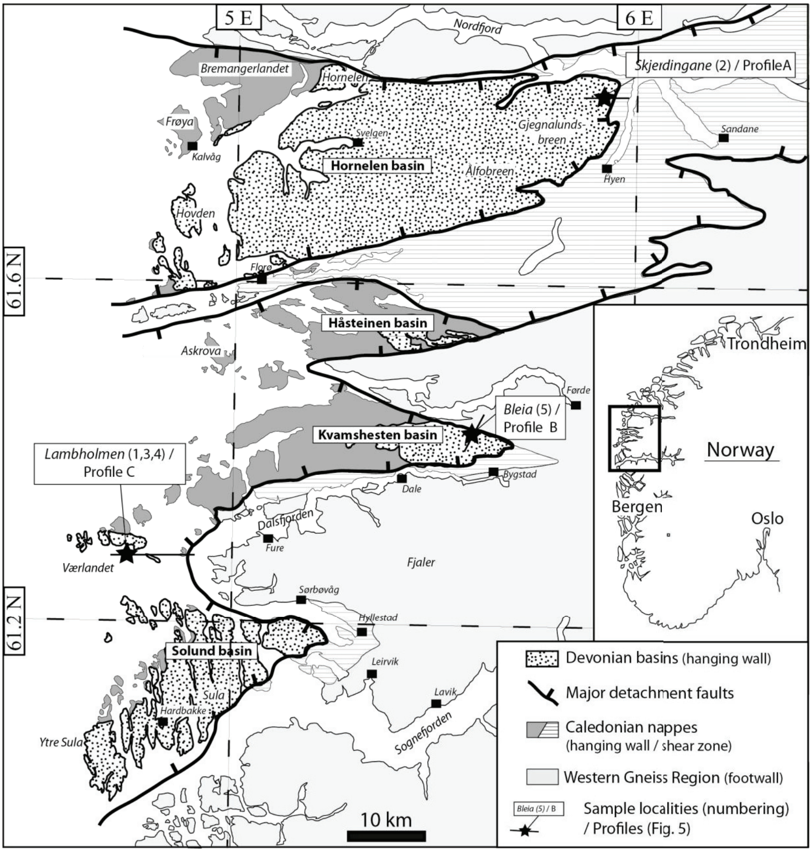

Fig. 1. Simplified geological map of western Norway showing the Solund, Kvamshesten, Håsteinen and Hornelen basins and the localities of the fossil-bearing sediments used in this study.

Table 1. RSCM thermometry results

Sample	Origin	Locality (unit)	Number of spectra	$RA1_{Lahfid}$	ε	$R2_{Beyssac}$	ε	T [°C]	ε
1	Our sampling	Lambholmen (Solund)	19	0.603	*0.002*	-	-	**284**	*±2.1*
2	*P000022**	Skjerdingane (Hornelen)	17	0.612	*0.002*	-	-	**295**	*±0.5*
3	Our sampling	Lambholmen (Solund)	13	0.615	*0.002*	-	-	**300**	*±1.9*
4	Our sampling	Lambholmen (Solund)	12	0.616	*0.003*	-	-	**301**	*±3.6*
5	*PTO157.257***	Bleia (Kvemshesten)	13	-	-	0.666	*0.004*	**345**	*±0.5*

The parameters $RA1_{Lahfid}$ (c.f. Lahfid *et al.* 2010) and $R2_{Beyssac}$ (c.f. Beyssac *et al.* 2002) are used to estimate temperatures respectively < 320 °C and > 330 °C. $RA1_{Lahfid}$, $R2_{Beyssac}$, and T are expressed in term of mean values of all the data with a standard error ε (= 1σ standard deviation divided by the square root of the number of measurements) within each sample. *Natural History Collections, University Museum of Bergen. **Natural History Collections, University Museum of Oslo.

250 ± 20 ^{o}C at a depth of 9.1 ± 1.6 km in the Hornelen and Kvamshesten basins to 315 ± 15 ^{o}C and a depth of 13.4 ± 0.6 km in the Solund basin. These data are taken to represent the regional metamorphism as a function of the burial of the basins. The new data presented here allow us to discuss the temperature of the basins not only as a function of burial depth, but also in relation to the distance from the NSDZ.

3. Methods

After sedimentation, the carbonaceous material (CM) trapped in the sedimentary protolith modifies its chemistry (carbonification during diagenesis), and then organises its internal structure (graphitization) under the effect of gradual heating during metamorphism (Beyssac *et al.* 2002). RSCM thermometry is based on the quantitative study of the degree of graphitization of CM, which is a reliable indicator of metamorphic temperature. Because of the irreversible character of graphitization, the CM structure is not sensitive to the retrograde overprint during exhumation of rocks and depends only on the maximum temperature reached during metamorphism (Beyssac *et al.* 2002). Temperature can be determined in the range 330–650 ^{o}C with a calibration-attached accuracy initially estimated to ± 50 ^{o}C, but re-estimated recently to ± 30 ^{o}C (Aoya *et al.* 2010). Relative uncertainties are, however, much smaller, in the range 10–15 ^{o}C (Beyssac *et al.* 2004; Negro *et al.* 2006). Recently, Lahfid *et al.* (2010) have demonstrated that the evolution of the Raman spectra of CM under low-grade metamorphism in the Glarus Alps (Switzerland) is highly correlated with the peak metamorphic temperature in the range of 200-330 ^{o}C. The results of this study is currently expanded and discussed for different tectonic settings allowing for testing and evaluating the respective roles of geothermal gradient(s), host rock lithologies or organic precursor as well as improving the temperature constraints. This detailed calibration shows that the correlation between the Raman spectra and temperature is systematic and that the RSCM thermometer may be extended to lower temperatures, in the range of 200-330 ^{o}C. In that purpose, the correlation obtained by Lahfid et al. (2010) in Glarus yields an excellent quantitative estimate of temperature. It is important to note that the fitting is different at low temperature compared to the original methodology by Beyssac *et al.* (2002), because the spectra are more complex with at least two more defect bands (Lahfid *et al.* 2010). Although elaboration of the definitive version of the quantitative calibration is still in progress, we used the qualitative evolution in Glarus based on the RA1 parameter (cf. Lahfid *et al.* 2010) as a first approximation to determine temperature values in the low-grade rocks (T < 330 ^{o}C). In Table 1 we provide a standard error on T, which is a proxy for the quality of the T data reflecting mostly the within-sample structural heterogeneity. The calibration-attached accuracy at low-T is similar to that at high-T around ± 30 ^{o}C.

Raman spectra were obtained using a Renishaw InVIA Reflex microspectrometer (IMPMC Paris). We used a 514 nm Laser Physics argon laser in circular polarisation. The laser was focused on the sample by a DMLM Leica microscope with a 100x objective (NA=0.85), and the laser power at the sample surface was set around 1 mW. The Rayleigh diffusion was eliminated by edge filters, and to achieve nearly confocal configuration the entrance slit was closed down to 15 µm. The signal was finally dispersed using an 1800 grooves per mm grating and analysed by a Peltier cooled RENCAM CCD detector. Before each session, the spectrometer was calibrated with silicon standard. Because Raman spectroscopy of CM can be affected by several analytical mismatches, we followed closely the analytical and fitting procedures described by Beyssac *et al.* (2002, 2003). Measurements were done on polished thin sections and CM was systematically analysed below a transparent adjacent mineral, generally quartz. 10 - 20 spectra were recorded for each sample in the extended scanning mode (700-2000 cm^{-1}) with acquisition times from 30 to 60 seconds. Spectra were then processed using the software Peakfit (Beyssac *et al.* 2003). Raman imaging was performed using the same configuration and the streamline mapping technology as described by Bernard *et al.* (2008).

4. Results

4.1. Presence of CM

To investigate the temperature conditions in the study area, we sampled from the base to the top across the stratigraphy within the Solund, Kvamshesten and Hornelen basins. Because of the eastward dip of the bedding in the basins, their stratigraphic base is generally several kilometres away from the NSDZ, whereas the highest stratigraphic levels in their eastern parts are at or near the detachment. In spite of careful and extensive sampling, we have been confronted with a systematic absence of CM from most of the fine-grained sand-, and siltstones. Disordered CM was indeed only found as big patches (Fig. 2.a) preserved in the lithologies containing macro-fossils of Devonian plants (Fig. 1). This CM is derived from original biological material trapped in the sediment and has been progressively transformed during burial. Presumably, such CM was originally present in most of the silt- and sandstones lithologies of the Devonian basins, and has later been removed by oxidation. Oxidation most likely occurred during the intense fluid circulation, which affected the basins after deposition (Svensen *et al.* 2001, Beinlich *et al.* 2010). Noticeably, we have observed the local presence of detrital graphite, which can be easily recognised through its flaky morphology and Raman signature (Fig. 2b, 2c, Fig. 4). Finding detrital graphite in such sediments is not a surprise as graphite may be massively recycled during erosion/deposition processes (Galy *et al.* 2008). This detrital graphite was observed either directly as flakes in the mineral matrix (Fig. 2b) or as inclusions within quartz grains (Fig. 2c). In some samples, detrital graphite was found in association with hematite (Fig. 4), which might set precise constraints on redox conditions that prevailed during the rock history. The redox conditions were oxidising enough to form hematite and to oxidise disordered CM, but not too oxidising to preserve detrital graphite. Graphite is by far less prone to oxidation than disordered CM because it has no chemical radicalisation and almost no nano-porosity allowing for fluid permeation (Galy *et al.* 2008).

Despite the large number of samples analyzed for this study (~50), our new temperature data are limited only to the fossil localities. Representative spectra for each sample are depicted in figure 3 and all measurements are listed in Table 1. Noticeably, the temperature data for each sample show high-internal consistency, with small within-sample structural heterogeneity of CM. In sample 5 from Bleia locality in the Kvamshesten basin, the CM is more graphitized and we therefore used the original RSCM calibration by Beyssac *et al.* (2002).

4.1. Temperature estimates

Our analyses give temperatures (± 30 ^{o}C) ranging from 284 ^{o}C to 345 ^{o}C in the different localities. These results indicate higher temperature in the Hornelen (295 ^{o}C) and in the Kvamshesten (345 ^{o}C) basins compared to the previous estimate of 250 ^{o}C for these units (Svensen *et al.* 2001). The new temperatures found in the Solund basin are lower, ranging between 284 ^{o}C and 301 ^{o}C, compare to the previous estimate of 315 ^{o}C. The standard errors reported in Table 1 reflect the homogeneity of the measurements of each sample. Therefore, the relative temperature variation between the different data points is well constrained within few degrees.

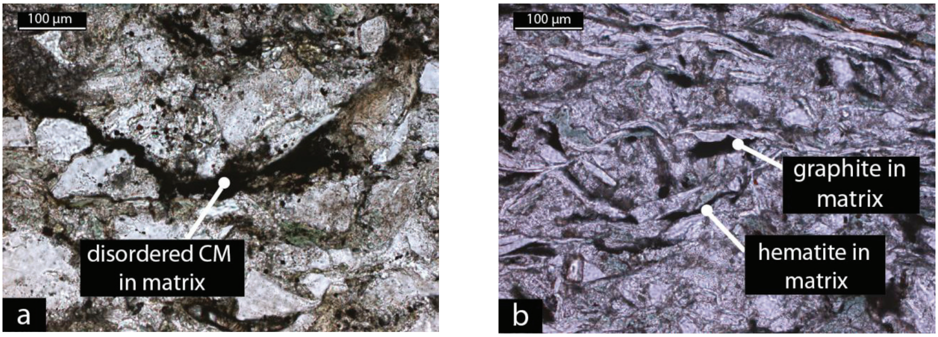

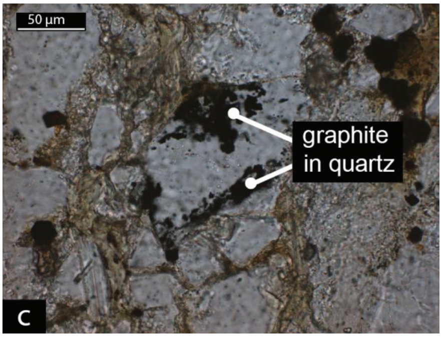

Fig. 2. a) Optical micrograph depicting disordered carbonaceous material from the north-western parts of the Solund Devonian basin at Lambholmen. b) Optical micrograph showing hematite associated with graphite in the mineral matrix of silty sandstone from the Hornelen basin (sample HOR23). c) Optical micrograph depicting graphite inclusions in clastic quartz grain from the north-western parts of the Solund Devonian basin at Lambholmen.

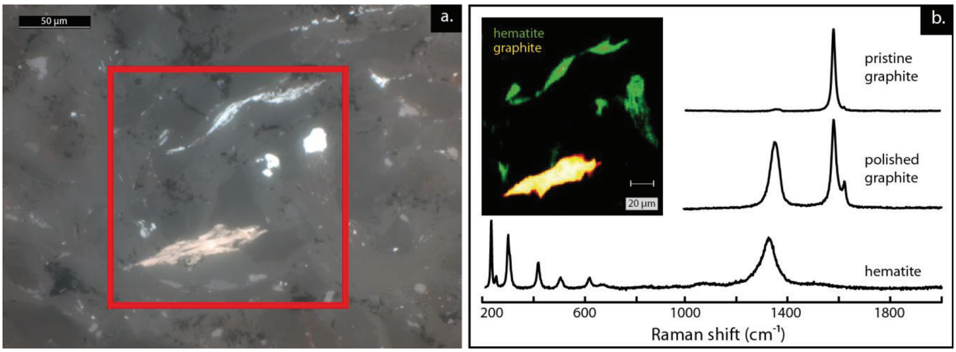

Fig. 3. a) Optical micrograph in reflected light showing hematite in association with a graphite flake in the mineral matrix of sample HOR23. The red box indicates the position of the Raman image presented in b). b) Right. Raman spectra of pristine graphite (measured below a transparent adjacent grain), polished graphite (measured at the surface of the thin section) and hematite. Note the strong effect of polishing which alters the structure of graphite and enhances the intensity of the main defect band. Left. Raman image obtained on image a) and evidencing the co-existence of graphite and hematite.

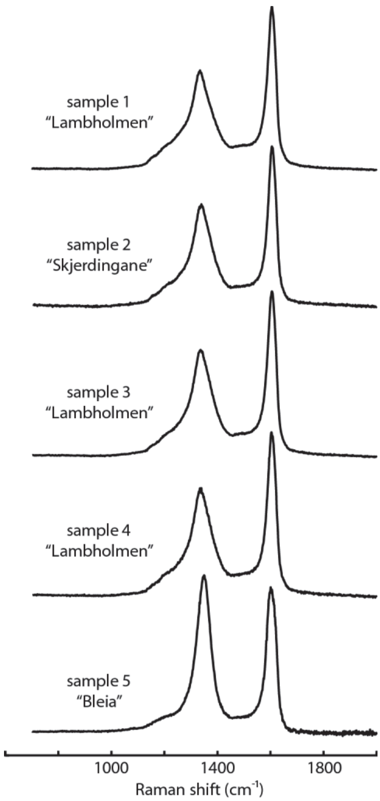

Fig. 4. Representative Raman spectra of disordered CM of the five samples containing plant fossil remains. The vertical axis corresponds to the signal intensity in an arbitrary unit.

5. Discussion

5.1. Comparison with previous work

To better compare our results with the previous estimates, we have reproduced the P-T and fluid inclusion isochores diagram (Fig. 5) for the basins from Svensen *et al.* (2001, p.67, Fig. 9). The new temperatures of our specific sample localities are shown and compared with the average metamorphic conditions given by this previous study. This diagram (Fig. 5) shows that our new data deviate from the regional metamorphic trend previously determined from the basins. In addition, it is noticed that the estimates of the average metamorphic conditions were based on analyses of veins found throughout the Solund and Hornelen basins, and in the central part of the Kvamshesten basin (cf. Svensen *et al.* 2001). Our samples are, in contrast, representative of specific localities in the basins: near the depositional unconformity for samples 1, 3 and 4, and close to the main detachment for the samples 2 and 5.

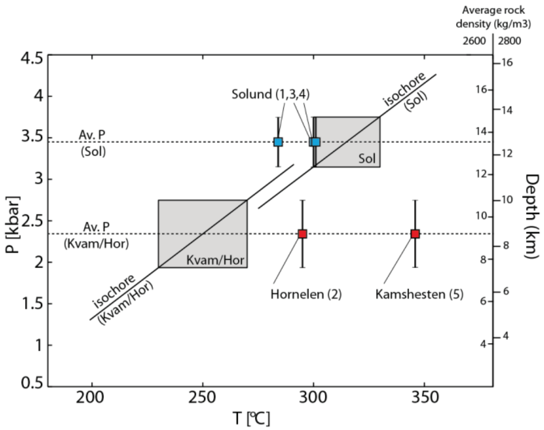

Fig. 5. P-T diagram from Svensen *et al.* (2001, p.67, Fig. 9). The solid lines are the fluid inclusion isochores from vein materials within the Kvamshesten, Hornelen (Kvam/Hor) and Solund (Sol) basins. The window shades represent the metamorphic conditions of the same respective units. The temperatures obtained in this study are plotted with the average pressure (av. P) of the different units (red/blue squares). A pressure-depth conversion scale is given on the right side of the diagram assuming overburden of constant rock density of 2600 and 2800 kg/m^3.

Two hypotheses can be put forward to explain the variation in temperature from the new data presented here.

1) *The variation between the previous estimates of the regional metamorphic temperatures and those reported from individual localities in our study, may suggest a difference in the burial depth at the present erosion level of the basins*. Using the result of 345 ^{o}C found near Bleia (sample 5, Kvamshesten basin), we can infer a local burial depth > 16 km for this locality. This estimate is obtained by projecting the temperature on the representative isochore (Kvam/Hor; see Fig. 5). This depth suggests a local burial of at least 6 km deeper than the average burial depth of the Kvamshesten basin. Several syn-depositional faults have been described in the basin (Osmundsen *et al.* 1998, 2000), but these cannot explain a differential burial of several kilometres in the area. We therefore exclude this hypothesis.

2) *The fast exhumation of the footwall of the NSDZ provided an additional heat source and thermally overprinted the basins during deposition and burial.*

The temperature within the basins may differ internally depending on the distance to the detachment fault. The NSDZ played a dominant role in the exhumation of high-grade Western Gneiss Region, crustal thinning as well as the formation of the Devonian basins in western

Norway. It is reasonable to assume that the juxtaposition of the warmer lower crustal rocks with the upper crust, including the basins, affected their respective thermal evolution. We consequently consider hypothesis 2 as the most appropriate to explain the variation of the data shown in figure 5. This interpretation is also supported by thermo-mechanical modelling of the geothermal field around large shear zones (Souche 2008).

The coherence of this preferred hypothesis is also supported by comparing the distances between the studied fossil localities and the detachment. The Lambholmen samples (1, 2, 4) in the northern Solund basin were taken at a low stratigraphic level and approximately 8 km from the NSDZ (Fig. 1). Sections with an average regional dip (~25^{o}) of the NSDZ (Hacker *et al.* 2003) suggest a vertical distance of approximately 3.5 km above the detachment for this locality (Fig. 6, profile A). Similar reconstructions show that the fossil localities at Skjerdingane at the uppermost stratigraphic level in the Hornelen basin (sample 3), and at Bleia near the detachment in Kvamshesten basin (sample 5) are at most 900 m above the detachment (Fig. 6, profile B and C). Therefore, the samples (3, 5) collected in the vicinity of the detachment may be warmer than the average regional metamorphism of the corresponding sedimentary rocks as indicated by the previous studies (Svensen *et al.* 2001). The samples (1, 2, 4) collected away from the detachment show an inverse relationship: they are colder than the average metamorphism. Our attempts to further constrain these relationships by systematic sampling across the stratigraphy of the basins have unfortunately not been successful because of the systematic absence of CM.

5.2. Heat from the NSDZ?

The progressive evolution of the NSDZ with gradual exhumation of the lower crust in the footwall can create an asymmetry of temperatures in the basin with an increase toward the detachment (Fig. 6). Several studies discuss the relevance of shear heating during large magnitude lithospheric deformation (e.g. Brun and Cobbold 1980; Burg & Gerya 2005; Leloup *et al.* 1999). Additional heat could be generated by deformation in large-scale shear zones, but the relative importance of this process remains mostly unquantified. Migration of fluids may also play a role in the thermal state of the basins by advecting heat. Detachments have long been described as structural pathways for channelling meteoritic water through the crust (Famin *et al.* 2004; Gottardi *et al.* 2011; McCaig 1988). However, an increase of temperatures in the basins is only possible if the rising fluids were exposed to a significantly

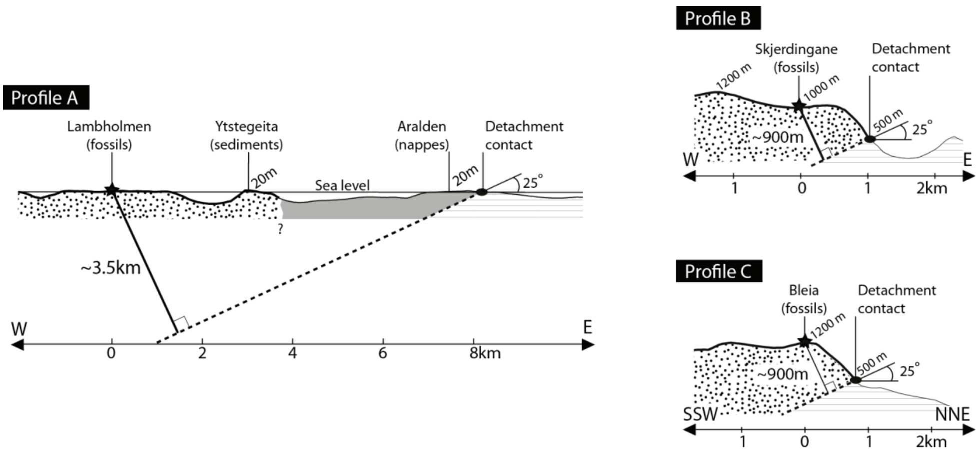

Fig. 6. Cross-sections showing structural position of the fossil-bearing localities above the NSDZ with an average dip of 25°. Topography and bathymetry along the profiles A, B and C (cf. Fig. 1) obtained from the map database at the Norwegian Geological Survey (http://www.ngu.no). The same legend as in Fig. 1 is used for the geological units.

warmer host in the shear zone or migrating from a deeper level in the footwall of the detachment.

5.3. Regional geotherm

The temperatures determined for the three largest Devonian basins of western Norway are important for estimating the regional geotherm. Previous estimates of the metamorphic conditions of the Hornelen/Kvamshesten and Solund basins suggested linear geotherms of *c.* 27 °C/km (250 °C at 9.1 km) and 23 °C/km (315 °C at 13.4 km), respectively (Svensen *et al.* 2001). The new temperatures determined by RSCM indicate additional heating in the vicinity of the detachment so that geodynamic processes perturbed the regional geotherm. If the new temperature estimates close to the detachment were part of a linear, steady state geotherm, it would require an 38 °C/km (345 °C for ~ 9 km burial), which by comparison with non-volcanic continental basins is considered too high.

5.4. Implications

The geology along the NSDZ records a setting where sediments were deposited near and partly in contact with a large-scale evolving detachment zone. The temperature in the north eastern margin of the Kvamshesten basin (and also in the Hornelen basin) is approximately 100 ^{o}C higher than the average temperature of the basins based on the estimates from vein-mineralogy and the authigenic minerals described from the sediments (Svensen *et al.* 2001). We suggest that a contact metamorphism-like process between the NSDZ, its footwall and the basin can explain this temperature anomaly. If shear heating contributed to the increase in temperature, it is possible that significant temperature anomalies may exist also elsewhere in similar structural settings. Rapid deformation within large shear zones may therefore have potential implications for thermal maturation of the above sedimentary basins.

6. Conclusion

We have presented new peak temperature estimates from the three largest Devonian basins of western Norway. The temperatures are internally consistent from several estimates at each individual locality, but show a significant regional variation between the different basins. The lowest temperatures are found near low stratigraphic level, near the depositional unconformity at the northwest margin of the Solund basin. The highest temperatures are found at high stratigraphic levels near the detachment along the eastern and northeast margins of the Hornelen and Kvamshesten basins respectively. This is in accordance with previous descriptions pointing to localized ductile shearing of conglomerates adjacent to the detachment fault. In order to explain the inverse temperature gradient with respect to the stratigraphy in the basin(s) we suggest that the very large and rapidly evolving NSDZ provided an additional heat source in the thermal budget of the basins. These lateral temperature variations cannot be explained by burial alone under a horizontally homogeneous geotherm. Our results illustrate the importance of considering the dynamic evolution of large-magnitude extensional shear zones to access the thermal history of above hangingwalls and supra-detachment basins.

Acknowledgments

This study was financed by the VISTA grant 6255. The Natural History Collections of the University Museum of Bergen and Oslo are thanked for providing some of the samples containing Devonian plant fossils. The study was carried out at a Norwegian Research Council Centre of Excellence: Physics of Geological Processes (PGP). The Raman spectrometer at IMPMC was funded by an ANR JCJC Grant (project GeoCARBONS, PI O. Beyssac).

References

Andersen, T. B., and Jamtveit, B. 1990. Uplift of deep crust during orogenic extensional collapse: A model based on field studies in the Sogn-Sunnfjord Region of western Norway. *Tectonics*, **9**, 1097-1111, doi:10.1029/TC009i005p01097.

Aoya, M., Kouketsu, Y., Endo, S., Shimizu, H., Mizukami, T., Nakamura, D., Wallis, S. 2010. Extending the applicability of the Raman carbonaceous-material geothermometer using data from contact metamorphic rocks. Journal of Metamorphic Geology, **28**, 895-914, doi:10.1111/j.1525-1314.2010.00896.x.

Beinlich, A., Austrheim, H., Glodny J., Erambert, M., Andersen, T. B. 2010. CO2 sequestration and extreme Mg depletion in serpentinized peridotite clasts from the Devonian Solund basin, SW-Norway. *Geochimica et Cosmochimica Acta,* **74**, 6935-6964, doi:10.1016/j.gca.2010.07.027.

Bernard S., Beyssac O. & Benzerara K. 2008. Raman mapping using advanced line-scanning systems: geological applications. *Applied Spectroscopy*, **62**, 1180-1188.

Beyssac, O., Goffé, B., Chopin, C., and Rouzaud, J. N. 2002. Raman spectra of carbonaceous material in metasediments: A new geothermometer. *Journal of Metamorphic Geology*, **20**, 859-871, doi:10.1046/j.1525-1314.2002.00408.x.

Beyssac O., Goffé, B., Petitet, J.P., Froigneux, E., Moreau, M. and Rouzaud, J.N. 2003. On the characterization of disordered and heterogeneous carbonaceous materials using Raman spectroscopy. *Spectrochimica Acta A*, **59**, 2267-2276, doi:10.1016/S1386-1425(03)00070-2.

Beyssac, O., Bollinger, L., Avouac, J-P., Goffe, B. 2004. Thermal metamorphism in the lesser Himalaya of Nepal determined from Raman spectroscopy of carbonaceous material. *Earth and Planetary Science Letters*, **225**, 233-241, doi:10.1016/j.epsl.2004.05.023.

Braathen, A., Osmundsen, P.T., Gabrielsen, R.H. 2004. Dynamic development of fault rocks in a crustal-scale detachment: An example from western Norway. *Tectonics*, **23**, TC4010, doi:10.1029/2003TC001558

Brun, J. P., and Cobbold, P. R. 1980. Strain heating and thermal softening in continental shear zones: a review. *Journal of Structural Geology*, **2**, 149-158, doi:10.1016/0191-8141(80)90045-0.

Burg, J. P., and Gerya, T. V. 2005. The role of viscous heating in Barrovian metamorphism of collisional orogens: thermomechanical models and application to the Lepontine Dome in the Central Alps. *Journal of Metamorphic Geology*, **23**, 75-95, doi:10.1111/j.1525-1314.2005.00563.x.

Cottle, J. M., Waters, D. J., Riley, D., Beyssac, O., and Jessup, M. J. 2011. Metamorphic history of the South Tibetan Detachment System, Mt. Everest region, revealed by RSCM thermometry and phase equilibria modelling. *Journal of Metamorphic Geology*, **29**, 561-582, doi:10.1111/j.1525-1314.2011.00930.x.

Eide, E. A., Torsvik, T. H., and Andersen, T. B. 1997. Absolute dating of brittle fault movements: Late Permian and late Jurassic extensional fault breccias in western Norway. *Terra Nova*, **9**, 135-139, doi:10.1046/j.1365-3121.1997.d01-21.x.

Famin, V., Philippot, P., Jolivet, L., and Agard, P. 2004. Evolution of hydrothermal regime along a crustal shear zone, Tinos Island, Greece. *Tectonics*, **23**, TC5004, doi:10.1029/2003TC001509.

Fossen, H. 2000. Extensional tectonics in the Caledonides: Synorogenic or postorogenic. *Tectonics*, **19**, 213-224, doi:10.1029/1999TC900066.

Fossen, H. 2010. Extensional tectonics in the North Atlantic Caledonides: A regional view. *Journal of the Geological Society, London,* Special Publications, **335**, 767-793, doi:10.1144/SP335.31.

Galy V., Beyssac O., France-Lanord C. & Eglinton T. 2008. Selective recycling of graphite during Himalayan erosion: a geological stabilisation of C in the crust. Science, **322**, 943-945, doi:10.1126/science.1161408.

Gottardi, R., Teyssier, C., Mulch, A., Vennemann, T. W., and Wells, M. L. 2011. Preservation of an extreme transient geotherm in the Raft River detachment shear zone. *Geology*, **39**, 759-762, doi:10.1130/G31834.1.

Hacker, B. R., Andersen, T. B., Root, D. B., Mehl, L., Mattinson, J. M., and Wooden, J. L. 2003. Exhumation of high-pressure rocks beneath the Solund Basin, Western Gneiss Region of Norway. *Journal of Metamorphic Geology*, **21**, 613-629, doi:10.1046/j.1525-1314.2003.00468.x.

Høegh, O. A. 1945. Contributions to the Devonian flora of western Norway III. *Norsk Geologisk Tidsskrift*, **25**, 183-192.

Jolivet, L., Goffé, B., Monié, P., Truffert-Luxey, C., Patriat, M., and Bonneau, M. 1996. Miocene detachment in Crete and exhumation P-T-t paths of high-pressure metamorphic rocks. *Tectonics*, **15**, 1129-1153, doi:10.1029/96TC01417.

Jolivet, L., Lecomte, E., Huet, B., Denele, Y., Lacombe, O., Labrousse, L., Le Pourhiet, L., Mehl, C. 2010. The North Cycladic Detachment System. *Earth and Planetary Science Letters*, **289**, 97-104, doi:10.1016/j.epsl.2009.10.032.

Kolderup, C. F. 1916. Bulandets og Værlandets konglomerat og sandstensfelt.: bergens Museums Aarbok 1915-16. *v. Naturvidenskabelig Række*, **8**, 1-26.

Kolderup, C. F. 1921. Kvamshestens devonfelt.: bergens Museums Aarbok 1920-21. *v. Naturvidenskapelig Række*, **4**, 1-96.

Kolderup, C. F. 1927. Hornelens devonfelt.: bergens Museums Aarbok 1926. *v. Naturvidenskapelig Række*, **6**, 1-56.

Labrousse, L., Jolivet, L., Andersen, T. B., Agard, P., Hébert, R., Maluski, H., and Schärer, U. 2004. Pressure-temperature-time deformation history of the exhumation of ultra-high pressure rocks in the Western Gneiss Region, Norway. *In*: Whitney, D.L., Teyssier, C. & Siddoway, C.S. (eds) *Gneiss Domes in Orogeny*. Geological Society of America, Special Papers, **380**, 155-183.

Lahfid A., Beyssac O., Deville E., Negro F., Chopin C. & Goffé B. 2010. Evolution of the Raman spectrum of Carbonaceous Material in low-grade metasediments: an example from the Glarus Alps (Switzerland). *Terra nova*, **22**, 354-360, doi:10.1111/j.1365-3121.2010.00956.x.

Leloup, P. H., Ricard, Y., Battaglia, J., and Lacassin, R. 1999. Shear heating in continental strike-slip shear zones: model and field examples. *Geophysical Journal International*, **136**, 19-40, doi:10.1046/j.1365-246X.1999.00683.x.

Lister, G. S., Etheridge, M. A., and Symonds, P. A. 1986. Detachment faulting and the evolution of passive continental margins. *Geology*, **14**, 246-250, doi:10.1130/0091-7613(1986)10<246:DFATEO>2.0.CO;2.

McCaig, A. M. 1988. Deep fluid circulation in fault zones. *Geology*, **16**, 867-870, doi:10.1130/0091-7613(1988)016<0867:DFCIFZ>2.3.CO;2.

McClay, Norton, M. G., Coney, P., and Davis, G. H. 1986. Collapse of the Caledonian orogen and the Old Red Sandstone. *Nature*, **323**, 147-149, doi:10.1038/323147a0.

McKenzie, D. 1978. Some remarks on the development of sedimentary basins. *Earth and Planetary Science Letters*, **40**, 25-32, doi:10.1016/0012-821X(78)90071-7.

Mulch, A., Teyssier, C., Cosca, M. A., and Vennemann, T. W. 2006. Thermomechanical analysis of strain localization in a ductile detachment zone. *Journal of Geophysical Research*, **111**, B12405, doi:10.1029/2005JB004032.

Negro, F., Beyssac, O., Goffe, B., Saddiqi, O., Bouybaouene, M. L. 2006. Thermal structure of the Alboran Domain in the Rif (northern Morocco) and the Western Betics (southern Spain). Constraints from Raman spectroscopy of carbonaceous material. *Journal of Metamorphic Geology*,**24**, 309-327, doi:10.1111/j.1525-1314.2006.00639.x.

Norton, M. G. 1987. The Nordfjord-Sogn Detachment, W Norway. *Norsk Geologisk Tidsskrift*, **67**, 93-106.

Osmundsen, P. T., Andersen, T. B., Markussen, S., and Svendby, A. K. 1998. Tectonics and sedimentation in the hangingwall of a major extensional detachment: The Devonian Kvamshesten Basin, western Norway. *Basin Research*, **10**, 213-234, doi:10.1046/j.1365-2117.1998.00064.x.

Osmundsen, P. T., Bakke, B., Svendby, A. K., and Andersen, T. B. 2000. Architecture of the middle Devonian Kvamshesten group, Western Norway: Sedimentary response to deformation above a ramp-flat extensional fault. *Geological Society, London*, Special Publications, **180**, 503-535, doi: 10.1144/GSL.SP.2000.180.01.27.

Osmundsen, P. T., and Andersen, T. B. 2001. The middle Devonian basins of western Norway: Sedimentary response to large-scale transtensional tectonics? *Tectonophysics*, **332**, 51-68, doi:10.1016/S0040-1951(00)00249-3.

Osmundsen, P. T., Braathen, A., Sommaruga, A., Skilbrei, J. R., Nordgulen, Ø., Roberts, D., Andersen, T. B., Olesen, O., and Mosar, J. 2005. Metamorphic core complexes and gneiss-cored culminations along the Mid-Norwegian margin: an overview and some current ideas, *Norwegian Petroleum Society*, Special Publications, **12**, p. 29-41, doi:10.1016/S0928-8937(05)80042-6.

Seranne, M., and Seguret, M. 1987. The Devonian basins of western Norway: tectonics and kinematics of an extending crust. *Geological Society, London,* Special Publications, **28**, 537-548, doi:10.1144/GSL.SP.1987.028.01.35.

Seranne, M., Chauvet, A., Seguret, M., and Brunel, M. 1989. Tectonics of the Devonian collapse-basins of western Norway. *Bulletin de la Société Géologique de France*, **5**, 489-499.

Smethurst, M. A. 1990. Palaeomagnetism of the Kvamshesten and Hornelen Old Red Sandstone Basins, western Norway. *Geophysical Journal International*, **102**, 585-601, doi:10.1111/j.1365-246X.1990.tb04585.x.

Souche, A. 2008. *Thermal evolution in the hanging-wall of a low angle normal fault: A finite element study of the Nordfjord Sogn Detachment Zone*. Unpublished Master thesis, Strasbourg Louis Pasteur University.

Steel, R. J., Mæhle, S., Nilsen, H., Røe, S. L., and Spinnanger, A. 1977. Coarsening-upward cycles in the alluvium of Hornelen Basin (Devonian) Norway: Sedimentary response to tectonic events. *Geological Society of America Bulletin*, **88**, 1124-1134, doi:10.1130/0016-7606(1977)88<1124:CCITAO>2.02CO;2.

Svensen, H., Jamtveit, B., Banks, D. A., and Karlsen, D. 2001. Fluids and halogens at the diagenetic–metamorphic boundary: evidence from veins in continental basins, western Norway. *Geofluids*, **1**, 53-70, doi:10.1046/j.1468-8123.2001.11003.x.

Torsvik, T. H., Sturt, B. A., Ramsay, D. M., Bering, D., and Fluge, P. R. 1988. Palaeomagnetism, magnetic fabrics and the structural style of the Hornelen Old Red Sandstone, western Norway. *Journal of the Geological Society, London*, **145**, 413-430, doi:10.1144/gsjgs.145.3.0413.

Torsvik, T. H., Sturt, B. A., Swensson, E., Andersen, T. B., and Dewey, J. F. 1992. Palaeomagnetic dating of fault rocks: evidence for Permian and Mesozoic movements and brittle deformation along the extensional Dalsfjord Fault, western Norway. *Geophysical Journal International*, **109**, 565-580, doi:10.1111/j.1365-246X.1992.tb00118.x.

Wernicke, B. 1985. Uniform-sense normal simple shear of the continental lithosphere. *Canadian Journal of Earth Sciences*, **22**, 108-125, doi:10.1139/e85-009.

Wernicke, B. 2009. The detachment era (1977-1982) and its role in revolutionizing continental tectonics. *Geological Society, London*, Special Publications, **321**, 1-8, doi: 10.114/SP321.1.

Paper II: Shear heating in extensional detachments: implications for the thermal history of the Devonian basins of western Norway

Manuscript submitted to *Tectonophysics*

Paper III: Modelling thermal convection in supra-detachment basins: example from western Norway

Manuscript prepared for submission to *Geofluids*

Annex paper: Influence of ice sheet and glacial erosion on passive margins of Greenland

Manuscript submitted to *Geomorphology*

Influence of ice sheet and glacial erosion on passive margins of Greenland

Sergei Medvedev[1], Alban Souche[1], Ebbe. H. Hartz[2,1]

[1] Physics of Geological Processes, University of Oslo, Blindern, 0316 Oslo, Norway

[2] Det norske oljeselskap, Bryggetorget 1, Aker Brygge, 0250 Oslo, Norway (Ebbe.Hartz@detnor.no)

Abstract

The presence of Mesozoic and Cenozoic marine sediments at an altitude of 1.2 km near Scoresby Sund (central East Greenland) and Nuusuaq peninsula (central West Greenland), and even up to 2 km in the Kangerdlugssuaq region (south central East Greenland), illustrate significant uplifts of Greenland's margins. The magnitude of these uplifts contrast somewhat with the absence of major tectonic activity along Greenland margins during the Cenozoic. In this study we test how much these vertical motions can be explained by glacial processes. We analyze the influence of the ice sheet loading in the central part of Greenland and the carving of the fjord systems on the evolution of the topography by numerically modelling these processes backward in time. In our experiments we start with the actual topography and ice thickness and evaluate the pre-glacial topography calculating the flexural isostatic response to unloading the ice sheet. By restoring "erosion backward in time" and calculating the flexural isostasic effects we estimate the influence of glacial carving and evaluate the pre-erosional topography of Greenland. Our analyses show that: (1) The load of the ice sheet causes up to 800 m subsidence of the bedrock topography of the central part of Greenland. (2) The peripheral bulging caused by this ice loading has a negligible effect on amplitude of the uplifted Greenland margins. (3) Glacial carving and corresponding development of the large fjord system has a significant influence on vertical motion of passive margins of central (east and west) Greenland and can explain up to kilometer scale vertical motions. (4) The models show, however, that much of Greenland's topography is not caused by ice-related processes, and thus origin of these older mountain chains remains enigmatic. (4) Masses eroded from the regions of significant glacial erosion are larger than the recognized amount of sediments

within adjacent off-shore basins, meaning that either the topography of those margins formed before break-up of Greenland or that sediments can move far away by the ocean. We also illustrate that our estimations are conservative because of low resolution of DEM used for calculations. Higher DEM resolution may increase effects off glacial carving by up to 40%.

1. Introduction

The interplay between the thick ice sheet, glacial erosion and bedrock surface of Greenland is intriguing, simply because of the size of the affected area and volumes of ice and rock involved. Thus we can expect tectonic scale amplitude of response to such interaction. Figure 1a illustrates the major masses of ice stored within the Greenland Ice Sheet now. We also can observe the traces of previous activity of ice shaping the margins of Greenland by carving out the fjord systems (Figure 1b).

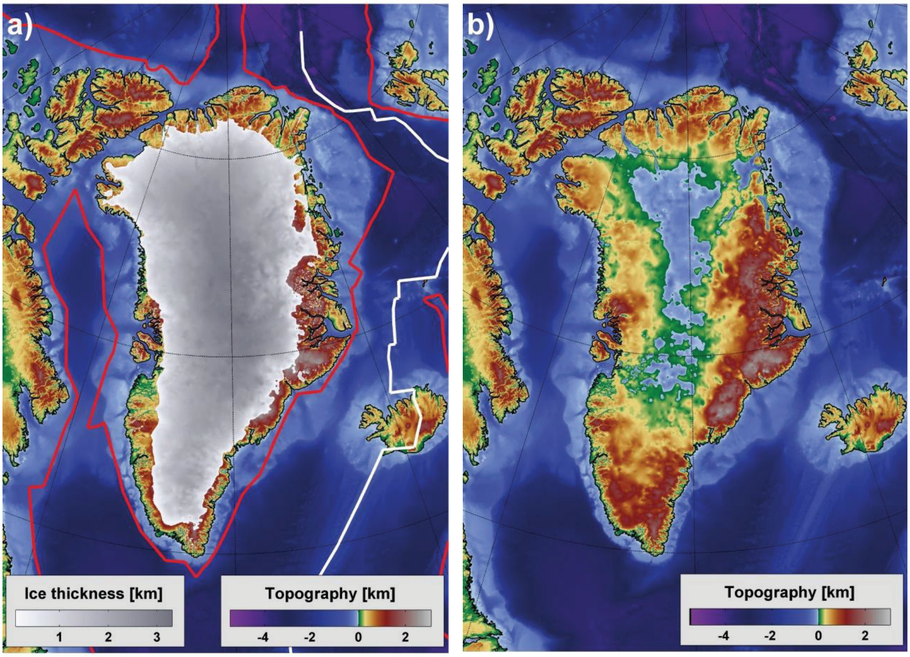

Figure 1. Map view on the study area (a) topography of the region with ice sheet thickness indicated by gray scale (the ice sheet of thickness more than 100 m is presented). Red lines present continent-ocean boundary, white line separates plates (after Muller et al., 2008). Note that some of the large sedimentary fans, building out from the mount of fjords, extend on to oceanic crust. (b) Bedrock topography.

Greenland displays a distinct topography with a central depression, surrounded by a near-continuous mountain chain along its coast. The nature of these mountains is enigmatic, given that the Mid Paleozoic orogeny of East Greenland was the last major orogenic event in Greenland (Henriksen, 2008; Wilson, 1966). After that time the Caledonian mountains first eroded and the topography was first filled with continental deposits, and later in the Permian to Mesozoic the future margins of Greenland were mostly submerged, as recorded in well exposed marine deposits now uplifted to mountains (Haller, 1971; Henriksen, 2003; Henriksen, 2008; Japsen and Chalmers, 2000). Both the western and eastern margin of Greenland record continental rifting, particularly in the Late Jurassic to Early Cretaceous prior to the Paleogene break-up of the North Atlantic. The break up is generally marked by thick layers of basalt, well exposed in both central west and east Greenland. During the Early Cenozoic Northern Pangea broke up leaving Greenland as a huge microcontinent between North America and Eurasia (Figure 1a; Bullard et al., 1965; Mosar et al., 2002). During this event Greenland was displaced northwards relative to the adjacent plates (Tessensohn and Piepjohn, 2000), resulting in transpressional deformation (fold and thrust belts) both between NW Greenland (Oakey and Stephenson, 2008) and North America, and NE Greenland and Svalbard/Eurasia (Leever et al., 2011). Therefore North Greenland displays active margins in the Cenozoic, whereas the margins south of these northern corners are truly passive. In the mid Cenozoic opening west of Greenland ceased, about the same time that central East Greenland passed above the Iceland Hotspot, and the Jan Mayen microcontinent shifted plate from Greenland to Eurasia (Figure 1a; Gaina et al., 2009; Lawver and Muller, 1994).

The modern landscapes of the peripheral part of Greenland are characterized by large fjord systems formed by glacial erosion (e.g., Odell, 1937), locally cutting more than 3 km down from the palaeo-surfaces. Figure 2 shows examples from the Scoresby Sund area in central east Greenland. Bonow et al. (2006) presents study of palaeo-plateau in the western Greenland, which was cut and tilted during Cenozoic. Erosion processes can be a major mechanism to enhance relief (Gilchrist and Summerfield, 1990, 1991; Molnar and England, 1990). Combined effect of localized erosion and diffused action of flexural isostasy may result in non-uniform evolution of the topography. Series of recently developed models of flexural isostasy attempt to explain the importance of the surface denudation and resulting isostatic uplift for different geological structures (Champagnac et al., 2007; Champagnac et al., 2009; Medvedev et al., 2008; Pelletier, 2004; Stern et al., 2005).

In this study we expand the local model of Medvedev et al. (2008) onto the entire Greenland realm (Figure 1). Medvedev et al. (2008) demonstrated how the carving of fjords and valleys of central East Greenland explains up to 1.1 km of uplift, which also is the maximum elevation of marine Mesozoic sediments of the area. By similar modelling we test to what degree this process is applicable to the entire Greenland. Considering a region which is much larger than one discussed in Medvedev et al. (2008), we remove the influence of boundary effects and analyze the degree of ice influence on the different parts of Greenland within the same model.

We first test how the loading of the ice sheet changes the topography of the region. Then we introduce the concept of erosion backward in time and present the results for the entire Greenland. A zoom of our results onto east and west margins of central Greenland gives numerical estimations of the influence of ice load and carving on the evolution of local topography. We also attempt to evaluate the balance of the erosional products outside the fjords with the topographic cavities inland, checking if one can find correlation in time and space between erosion and deposition.

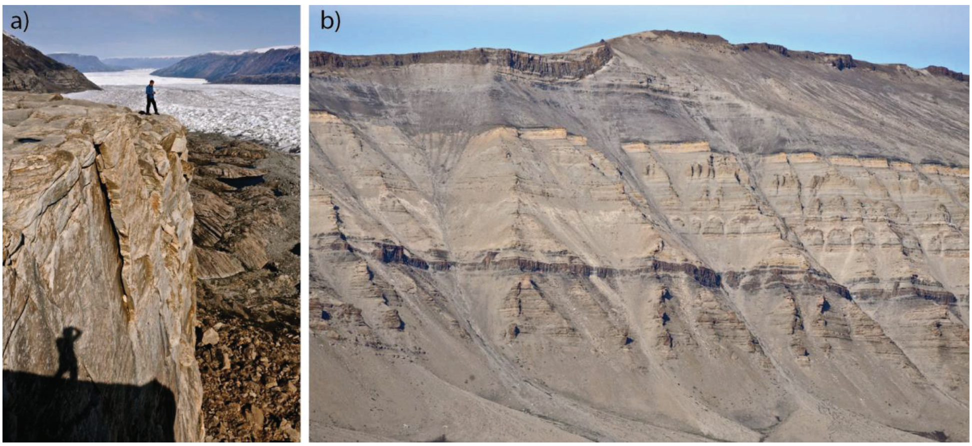

Figure 2.(a) Palaeo surface of East Greenland cut by glaciers/fjords. The darker ice is Vestfjord Glacier, whereas the lighter ice is the sea ice of Vestfjord (part of Scoresby Sund fjord system). (b) Mafic sill intrusions imbedded into marine Jurassic deposits on Southeastern Jameson Land. The two sills, dark layers on low central and top of the ca. 500 m cliff, make up approximately 10% of the rock volume. Locations of photographs are marked on Figure 9a.

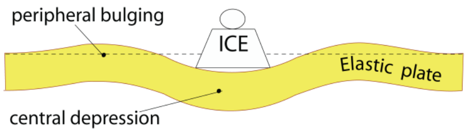

Figure 3. Cartoon view on the effects caused by loading of ice sheet on Greenland topography. Combined effects of loading, isostasy and flexural rigidity of the lithosphere may result in significant central depression and peripheral bulging.

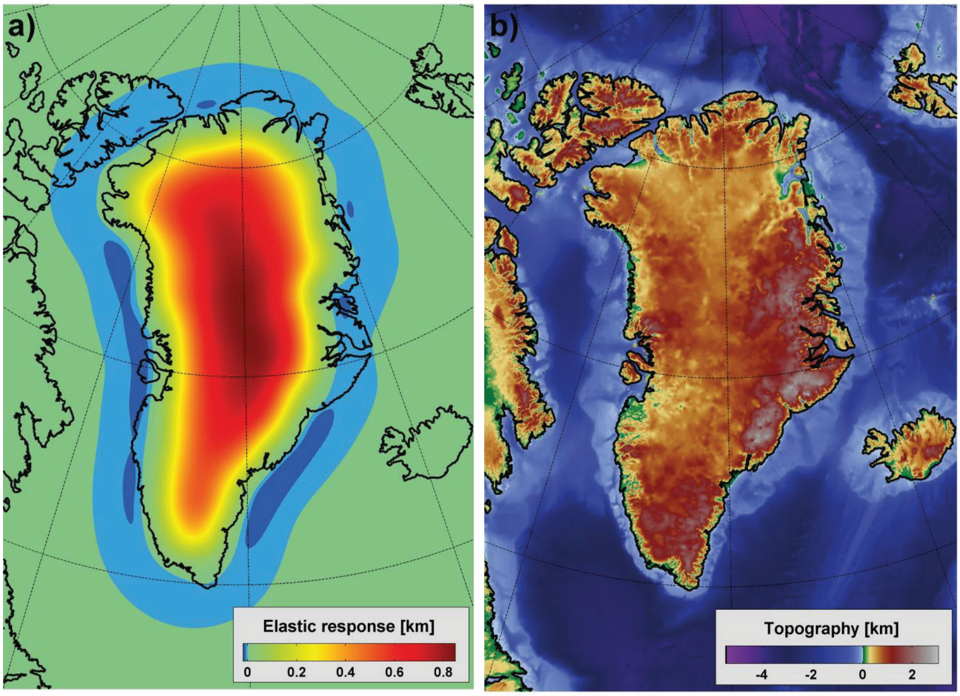

Figure 4. Results of numerical experiment of removing the ice sheet load. (a) The elastic response indicates significant (0.8 km and higher) central uplift but insignificant (less than 20 m) peripheral bulging. (b) Bedrock topography of Greenland isostatically adjusted after removal of the ice sheet (cf. Figure 1b). The calculations were performed using EET=20 km and ETOPO1 topography and ice thickness. The variations of the parameters and DEM's do not affect the conclusions. This configuration is used as initial position for calculations of next parts of the study.

2. Influence of load from Greenland ice sheet

The Greenland Ice Sheet exceeds 3 km in thickness, and covers most of Greenland (Figure 1a). The bedrock topography of Greenland (Figure 1b), resemble that of a typical response of an elastic plate subjected to a load in its central part (Figure 3). The significance of this effect is numerically investigated in the case of Greenland by removing the equivalent weight of the ice sheet and numerically calculating the flexure of the lithosphere due to the corresponding isostatic response.

The numerical model utilizes Matlab-based numerical suite ProShell (Medvedev et al., 2008). The model uses two grids, one for the surface loads integration and another for calculation of the elastic response. Resolution of topographic grid is 1.5 km, whereas elastic calculations were mainly performed using 7.5 km grid resolution. We check different resolutions to ensure durability of modelling. We also checked the model results for a range of elastic thickness (EET) values, 15, 20, and 30 km. The ice density used 930 kg/m^3 and mantle density is 3300 kg/m^3.

The input topographic data used in this work are taken from three different digital elevation models, ETOPO2 (developed by the US National Geophysical Data Center), ETOPO1 (Amante and Eakins, 2009), and SRTM30 (Becker et al., 2009), although we do not discuss results obtained using ETOPO2 as its resolution is too low. Results based on different DEM were compared for durability. All the global data sets are not exact, especially in the remote areas like one discussed here. Data on ice thickness is taken from ETOPO1 and from Bamber et al. (2001). In many places within our model domain the date sets show significant differences (with topography differences up to 600 m and ice thickness data of up to 200 m). We performed careful comparison of results to ensure that our conclusions do not depend on a particular choice of data set.

The results of the calculations show that the central part of Greenland responses significantly (up to ~850 m) to the unloading of the ice cap, whereas the associated peripheral bulging is only of few meters (less than 20 m). Most of the peripheral bulging occurs offshore. The Scoresby Sund fjord system and the Disko island are the two regions where the peripheral bulging could potentially affect inland topography but the computed amplitude of the uplift is negligible. Thus, elastic bulging of the lithosphere due to the ice loading contributes too little to be considered as one of the major mechanisms controlling the uplift of mountains around Greenland ice sheet.

3. Influence of Glacial erosion: general results

The topography obtained after removal of the ice sheet (Figure 4b) is used as input topography for the numerical experiments of this section. Here we attempt to estimate the influence of the erosional carving along the fjord systems. To this end, we model the erosion processes backward in time (Figure 5).

Erosion, especially glacial carving, locally removes material from the surface and unloads lithosphere activating the buoyancy forces from the deeper Earth (Figure 5a-b). These forces, acting on the effectively elastic lithosphere, trigger isostatic elastic uplift of the lithosphere. The horizontal extend of such uplift is usually larger than the scale of the erosion localized, e.g., within fjords, and thus isostatic readjustment may result in topographic uplift of surrounding non-eroded areas (Figure 5c). Note that removing material by erosion will always reduce the average elevation of the subjected area, and uplift may be found only locally.

Quantifying erosional processes is possible only if the initial landscape is known. In our experiments we assume that by numerically filling the eroded places with crustal material and adjusting it isostatically, we can estimate the elastic response and potential vertical movements of surface topography backwards in time (Figure 5d-f).

The numerical filling of the fjords and corresponding isostatic readjustment (the erosion backward in time) go iteratively. The procedure affects on-shore regions between the main mountain chains and modern shoreline. On each iteration step we find concavities (simply the points within the rectangular mesh with elevation below the average of the four neighbors) and add slightly less material (with density of crustal rocks 2800 kg/m^3) than required to equalize topography with neighbors' average. While the redistribution of material is processed on the topographic mesh, the associated isostatic response is calculated on the elastic plate and is assumed to be immediate. We repeat this process until no more sensible changes happen to the landscape.

To reduce the number of parameters in the model, we assume that the elastic property of the lithosphere is described by a thin elastic plate with uniform thickness for the entire model domain (Figure 1). We compare calculations based on EET ranging between 15 and 30 km.

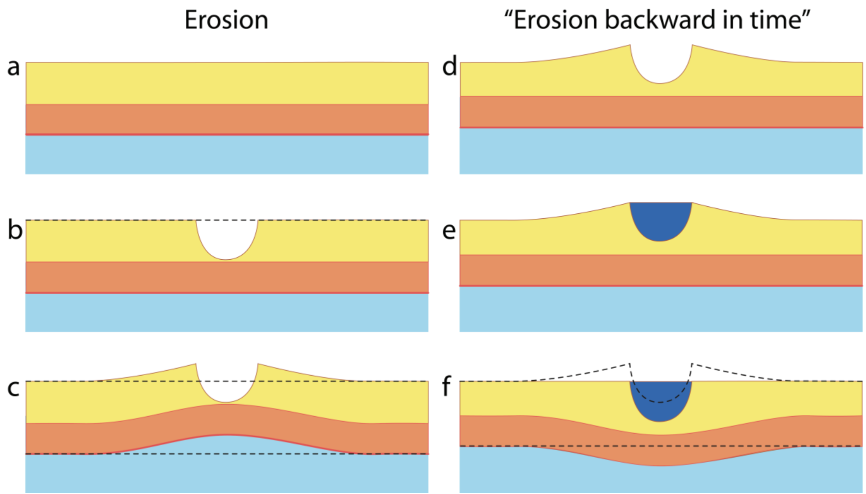

Figure 5. Illustration of how erosion reshapes topography (a-c) and the model approach of this study, "erosion backward in time" (d-f). We consider a simple three-layer lithosphere (not to vertical scale) with an upper layer (yellow) passively sitting on top of an elastically strong part of lithosphere (orange) which in turn underlined by an inviscid asthenosphere (gray). The initial surface (a) is subjected to localized erosion (b) which unloads lithosphere and thus results in isostatic uplift (c). In the "erosion backward in time" the localized eroded areas are assumed as areas with concave shape (d) which we numerically fill with bedrock material (e) and then calculate the downward motion due to the additional load (f). We assume that absolute values of vertical motions on (c) and (f) are approximately equal.

Even though the results in general do not vary significantly (only several tens of meters in the local uplift) and do not alter the main conclusions, some regional-scale observations match quantitatively better to model with EET=15 km (central west Greenland) and EET=20 km (central east Greenland). For the sake of simplicity we did not consider models with variable EET, which would introduce additional degree of uncertainty in the model and do not change first-order conclusion, but rather compare local observations with model results inferred from models of uniform plate property of corresponding EET.

Figure 6 presents results of calculations for the case of effective elastic thickness of the lithosphere of 20 km. Significant amount of placed-in material (Figure 6a, up to 3.1 km) is observed mainly along the major fjords of Greenland and result in significant isostatic flexure of the lithosphere (Figure 6b, up to 1.2 km in amplitude). We can consider the resulting smooth landscape as the approximation to the pre-erosional landscape of Greenland generated by the model (Figure 6c).

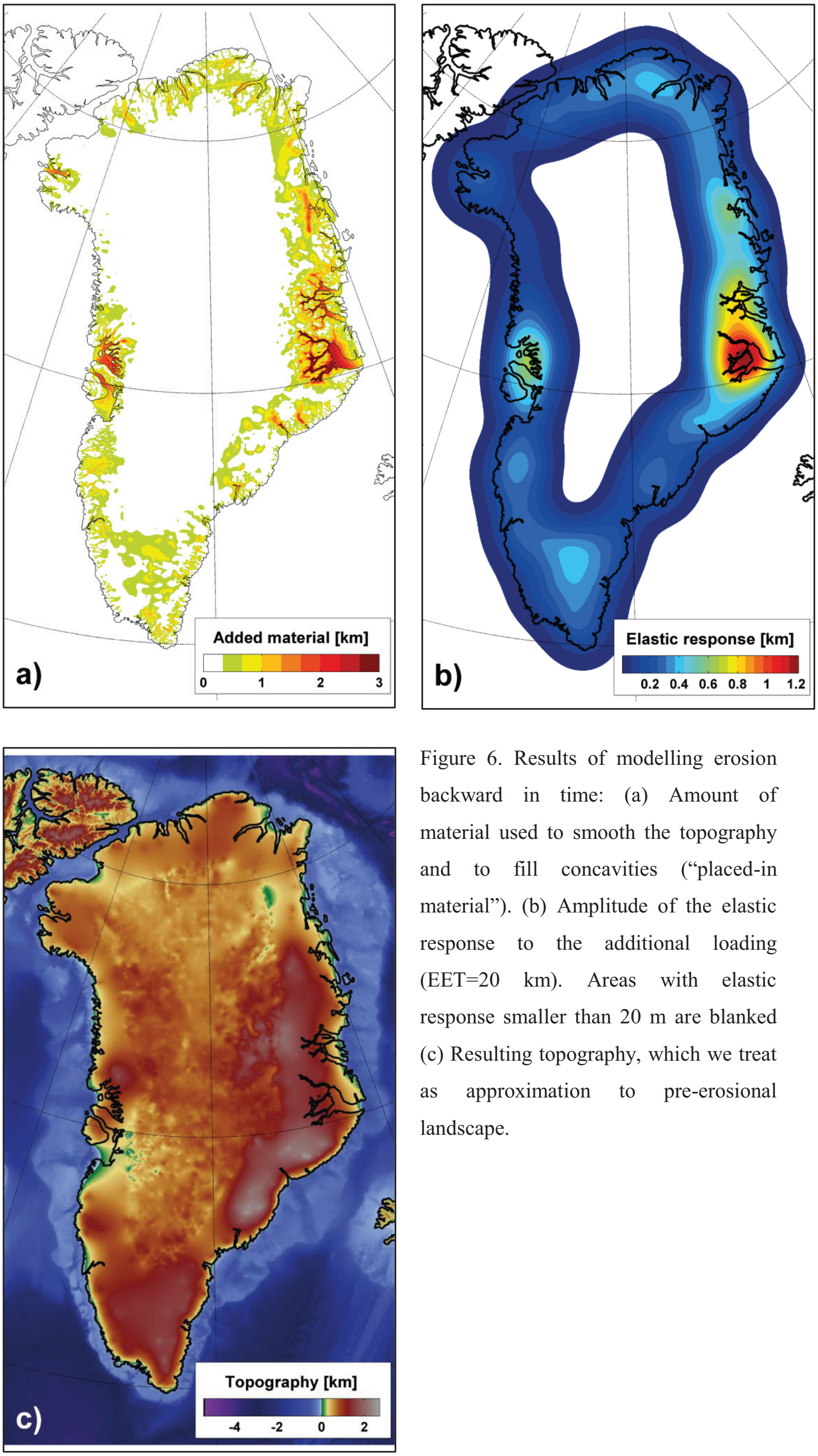

Figure 6. Results of modelling erosion backward in time: (a) Amount of material used to smooth the topography and to fill concavities ("placed-in material"). (b) Amplitude of the elastic response to the additional loading (EET=20 km). Areas with elastic response smaller than 20 m are blanked (c) Resulting topography, which we treat as approximation to pre-erosional landscape.

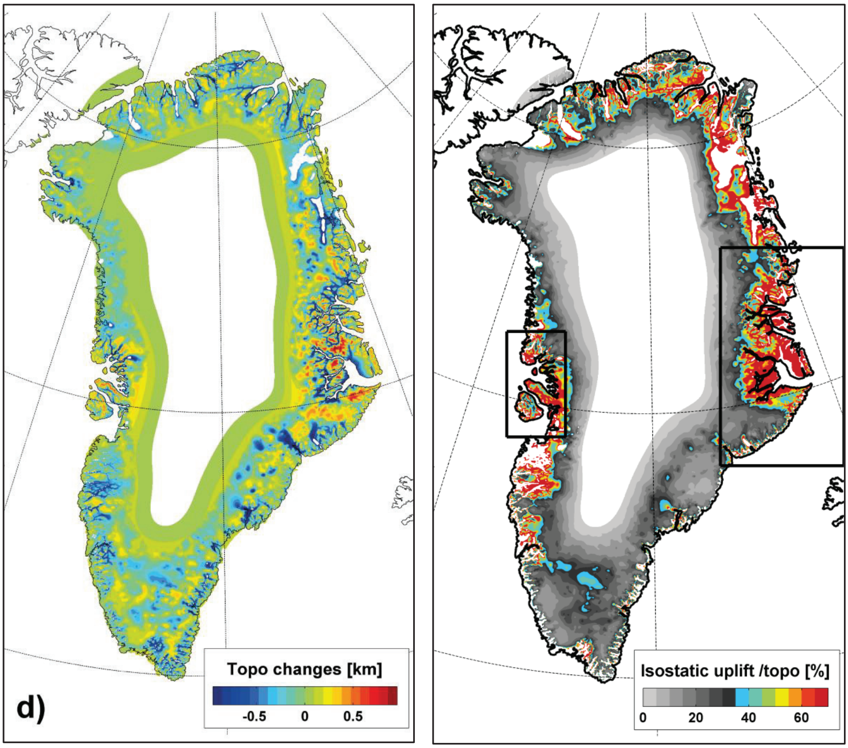

Figure 7. Interpretation of model results: (a) Topography changes due to erosion [=pre-glacier topography (Figure 4b) – modelled pre-erosional topography (Figure 6c)]. (b) Ratio between elastic response and present-day topography. Areas with topography below 200 m and with an elastic response smaller than 20 m are blanked. Black squares outline regions discussed in more detail in the remainder of this study.

As discussed above (e.g., Figure 5), adding material to the upper surface not only elevate topography, but locally may result in decrease in elevation as shown by Figure 7a. The results also show that the erosional processes do not create the main mountain belt in Greenland, as the pre-erosional mountains are of the similar elevation.

To assess the results we compare our Greenland-scale model with observations on a regional scale. Figure 7b presents ratio of modern topography (Figure 4b) to the elastic response due to erosion (Figure 6b). This ratio renders regions where isostatic movements are in the same order as the elevation of the topography. It highlights regions where uplift may potentially caused by glacial erosion and allows us to choose two areas to discuss in detail in the next sections (Figure 7b). Other areas also demonstrate the high ratio, but they are either of insignificant topography (areas south from western square and north from eastern square on

Figure 7b), or subjected to complex tectonic evolution during Cenozoic (northern Greenland, Oakey and Stephenson, 2008, Leever et al., 2011). Note that to ensure general approach and to avoid influence of unknown boundary conditions on the numerical models, we do not perform special regional modelling, but zoom in the results of the calculations of this section onto two chosen regions.

Thus, by modelling the effect of glacial erosion of the entire Greenland, we have been able to estimate the topography and isostatic evolution and present the model for pre-erosion landscape. We also show that two particular regions are potentially more influenced by this mechanism than the rest of Greenland.

4. Influence of ice sheet and glacial erosion: close up on Central West Greenland

The topography and geology of central west Greenland displays a highly incised enveloping surface with basalts covering Mesozoic marine sediments elevated high above sea level (Japsen et al., 2010). We compare the results of our global model with the regional study published in Bonow et al. (2006) with particular interest in profile B-B' of their study. This profile (Figure 8a) goes along the entire Nuussuaq peninsula. Bonow et al. (2006) point to the Mesozoic marine sediments at the elevation of more than 1 km and present the eastern part of profile as a remnant of a palaeo-plateau formed approximately at sea-level (Figure 8c). Why this plateau is now uplifted by almost 2 km and tilted westward by approximately 1.2 km remains enigmatic.

The topographic sampling performed in the regional study of Bonow et al. (2006) is much more precise than the data set used in our model (SRTM30), but despite this resolution gap, the topographic signature of the palaeo-surface olong the Nuussuaq peninsula is easily mapped in our model (Figure 8c).

Figure 8c shows that removing the ice sheet change elevation of the eastern part of the profile by approximately 100 m, as it is already discussed in Bonow et al. (2006). The erosion, however, have a much stronger influence on the topography evolution. The material added within our model restoring erosion backward in time is illustrated in figure 8c (blue fill). By restoring up to 1 km of erosion backwards in time, the profile is smoothed towards a plateau. However, the most significant downward motion of profile is caused by the regional isostatic response to filling (backwards in time) the fjords adjacent to Nuussuaq peninsula, Uummannaq and Vaigat, where the amount of material adds up to 3 km (Figure 8a).

Reversing the "backward in time" model we estimate the role of glacial erosion and ice loading within the evolution of landscapes of Nuussuaq peninsula and surrounding area. Significant glacial erosion results in carving the palaeo-plateau and uplifting it by up to 0.8 km (out of total 2 km). Additionally, uneven glacial erosion and ice loading contribute to east-ward tilt of the chosen profile by 0.5 km (out of total 1.2 km).

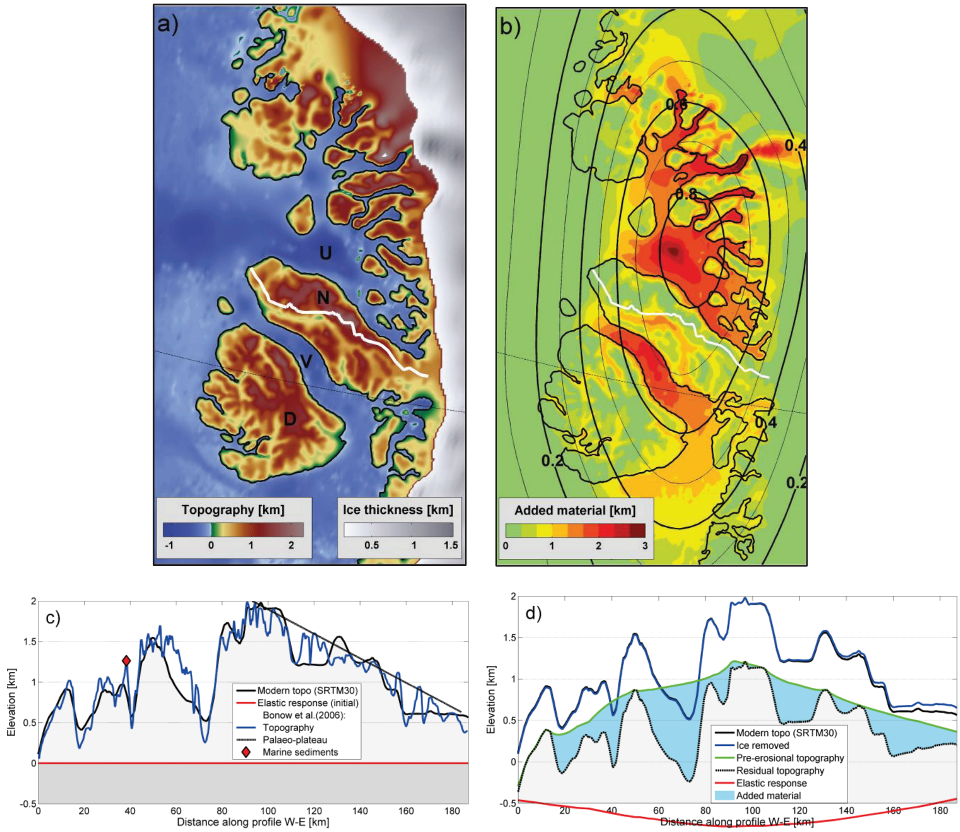

Figure 8. General view on the region with white line indicating the position of the profile considered (a). (b) Amount of added material during the modelling of the erosion backward in time, with isolines indicating regional elastic response in km (black) and the position of the profile considered after Bonow et al. (2006) (white). (c) Initial data along the profile (data from Bonow et al. (2006) separated at the bottom part of the legend) and (d) model results projected on the profile. Geographical locations on (a): D=Disko island, V= Vaigat strait, N= Nuussuaq peninsula, U= Uummannaq fjord.

The western part of profile shows presence of marine sediments at high elevation (1.2 km, Figure 8b). The total erosion-related uplift in that area (difference between green and blue lines on Figure 8c) is only 200 m. However, in this particular area the global DEM (SRTM30) used in the global model for Greenland, is rather inaccurate, and of low resolution. Thus the low (200 m) rise of the peak with marine sediments probably reflect data resolution used in numerical simulations. All other dominating peaks in the area have risen by approximately 700 m, which is more than half of the elevation of the marine deposits.

The results of this section show that the ice loading and glacial erosion contribute significant to reshaping the landscapes of the central west Greenland. The results presented in this section are based on DEM SRTM30 and effective elastic thickness of 15 km. Variations of data (using ETOPO1 and/or different elastic thickness) give similar results with quantitative effects within 10% difference.

5. Influence of glacial erosion on the evolution of Central East Greenland

The topography of central east Greenland is dominated by enormous fjord systems: Scoresby Sound, Kong Oscar Fjord and Kejser Franz Joseph Fjord (Figure 9a). The largest, Scoresby Sound, is approximately 400 km long, up to 60 km wide and at some places cuts more than 2 km high paleosurfaces (Figure 2a) to a depth of 1.5 km below sea level. Medvedev et al. (2008) pointed out that the mountains between fjords are almost as high as the adjacent main mountain chain, but are not supported by thickened roots (Schmidt-Aursch and Jokat, 2005) and that the high elevation of those mountains may be a result of significant erosion. The same mechanism was suggested to explain Mesozoic marine sediments uplifted up to 1.2 km in the ford area (Figure 2b, Henriksen, 2003).

The erosional unloading of this region has resulted in up to 1.1 km isostatic uplift (Medvedev et al., 2008). In the present study we revisit the area considering mainly the evolution of upper surface using the results obtained while modelling the entire Greenland. The result of the global model zoomed to the area indeed show that the elastic isostatic response, 0.4-1 km, may indeed explain the amount of uplift in the areas of Mesozoic marine sediments (Figure 9b). However, the model assumes filling up the concave shapes even on large scale and thus the pre-erosional landscape of the areas of marine sediments is well above sea level, even after applied isostatic readjustment. Although the pre-erosional elevation in those areas is not

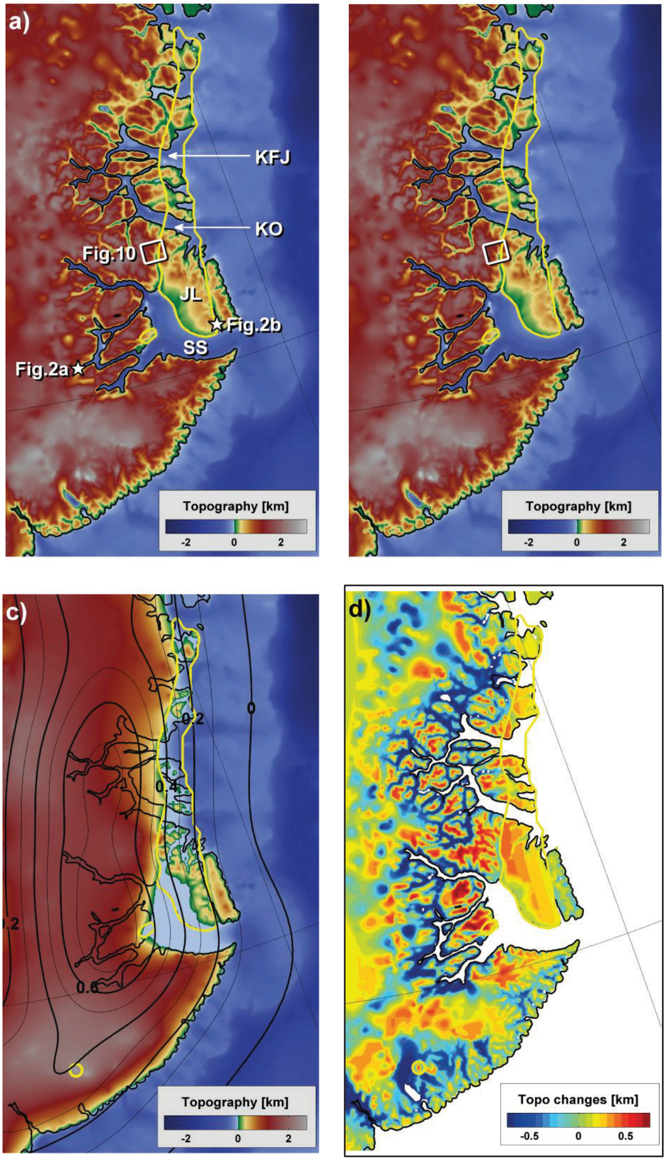

Figure 9. Results zoomed to central East Greenland. (a) The modern day topography. (b) Model results with colorcoding of the pre-erosional topography with black isolines of elastic response in km. (c) Results for the model with the special treatment of the marine sediments with black isolines of elastic response in km. Note that most of the marine sediments are below sea-level on (c). (d) Elevation changes due to erosion within modified model. Yellow line outlines the locations of marine sediments along east coast of Greenland (Henriksen, 2003) and in Kangerdlugssuaq area (Myers et al., 1988). White square in (a) shows location for analysis presented on Figure 10, white stars indicate locations of photographs Figure 2. Geographical locations on (a): SS = Scoresby Sund, Jl = Jameson Land, KO = Kong Oscar fjord, KFJ= Kajser Franz Joseph fjord.

high (mainly below 0.5 km), we cannot expect that marine sediments would be accumulated in such areas. To explain the uplift of marine sediments within our simple model we have to find an alternative approach.

The model presented in this study is based on elastic plate response to loading and unloading caused by glaciations and erosion. We also assume that the isostatic response is immediate (essentially assuming that asthenosphere underlying the lithosphere is inviscid). Thus, our model does not have explicit time-dependence. Moreover, the model is addictive in time and space: effects caused by loads separated by time and space can be calculated separately and the sum of responses is equal to response of summarized load. Thus we can suggest the model in which some parts of the Scoresby Sund area were eroded earlier than others.

In the modified model (Figure 9c and d) we assume that the landscape of the central east margin covered by marine sediments was formed earlier than the surrounded regions. This assumption is supported partially by study of Swift et al. (2008), who show that portions of landscapes in the area were developed before break-up of Greenland and Eurasia.

Figure 9 (c and d) present the results of the model in which the area characterized by Mesozoic marine sediments (within yellow line on the Figure 9) is subjected to erosion backward in time only if it is below sea level. The rest of the model (entire Greenland) is subjected to the same procedures as before (e.g., Figure 6). The elastic response in the area, even though still significant, becomes smaller (up to 0.7 km on Figure 9c vs. 1.2 km on Figure 9b). However, the resulting pre-erosional topography is almost entirely below sea level within area of marine sediments (with maximum topography of 0.5 km on Figure 9d vs. up to 1 km on Figure 9c). The load from the fjords fill within adjacent areas is enough to bring the margin with marine sediments under water within our “erosion backward in time” model; and thus erosion (considering real time evolution) results in uplift of marine sediments up to 300-600 m (Figure 9d).

Results presented in this section show that erosion of the central east Greenland margin may result in the uplift of the Mesozoic marine sediments of the area well above sea level. The preferred model requires that the landscape of the most outer part of the margin was formed prior to the internal part.

6. Discussion

In our calculations, based solely on geometrical definitions of concavities and immediate elastic response of the lithosphere, we cannot constrain the time of evolution. Post-processing of masses redistribution can give us time scale for the model. The model allows us to calculate the masses involved in the erosion process and compare it with amount of off-shore sediments, which we have attempted to average from published profiles of offshore Greenland (e.g., Berger and Jokat, 2009; Chalmers et al., 1993; Chalmers, 2000; Hamann et al., 2005; Japsen et al., 2006; Tsikalas et al., 2005). Even though the data on the amount of off-shore sediments is sparse, we may conclude that the masses eroded from the central east Greenland are much larger than amount of sediments accumulated in adjacent off-shore areas. Similar conclusion may be done for Western Greenland, but with less certainty, as the difference is not that great. Two obvious mechanisms may explain this inequality: (1) the eroded material travels long distance; and (2) the landscape was (partially) formed before break-up of surrounded oceans (Figure 1a). The latter mechanism is supported by geomorphological and stratigraphical studies of Swift et al. (2008) on the central east Greenland. However, exact quantitative analysis needs more data on the off-shore sediments.

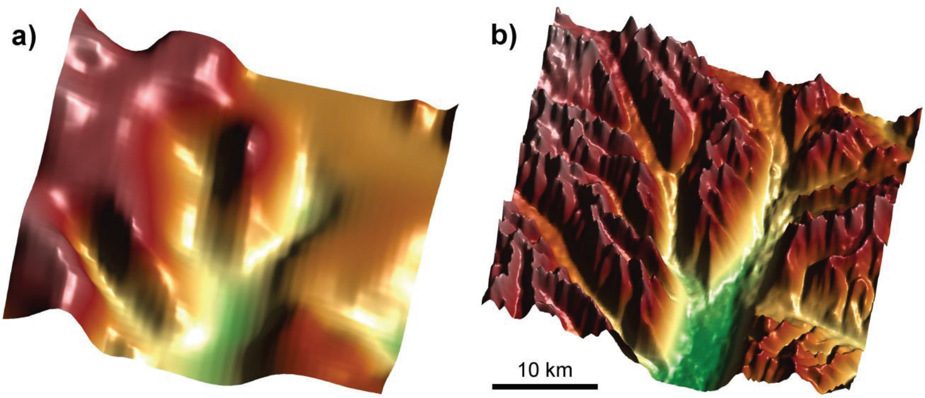

Figure 10. Examples of topography derived from two different data sets, (a) SRTM30 (resolution 30 arc seconds or 0.5-1 km) and (b) from Aster data set (resolution 1 arc second, approx. 30 m). We use SRTM30 and ETOPO1in our calculations because of lack of global data with high resolution (especially the lack of ice-thickness data). Vertical exaggeration is 10 times. Location of this example area is outlined on Figure 9a. The color-scale of these figures is the same as on all other topographic figures.

The model presented in this study might be highly sensitive to the resolution of the mesh used to calculate the topographic changes and the DEM. In the model we use SRTM30 and ETOPO1 data sets (approx. 1 km resolution) and the mesh resolution of 1.5 km is dense enough to catch the features of DEM. However, higher resolution topographic data would record more dramatic topography, which then give the model more cavities to fill and amplify the effect of isostatic response.

To test the sensitivity to topographic resolution we calculate the total volume trapped between the topography and the "convex envelope" in several sample localities in the Scoresby Sund area using different DEMs. Figure 10 demonstrates significant difference in topography of one sample area using SRTM30 and ASTER (Advanced Spaceborne Thermal Emission and Reflection Radiometer, a joining venture of METI and NASA) data (prepared by the NASA LP DAAC, USGS/EROS Center). In the areas of comparisons the high resolution data reveal 30 to 49% more space between the DEM and the enveloping surface. Most significant contribution to that difference brings higher topography variations (peaks are higher and valleys are deeper) within the higher resolution DEM (sf. Figures 10a and b). Thus, the erosional-related (un-)loading performed in this study and based on global DEM (Figure 10a) maybe significantly smaller than in reality.

We already discussed some specific problems of low resolution of our model when addressed marine sediments on the western part of the Nuussuaq peninsula profile (Figure 8b). Those marine sediments are located on the peak which simply does not exist in the DEM used here (SRTM30 in that case) and thus this significant uplift of marine sediments there cannot be discussed within the model.

Simplifications of our model and absence of the high-resolution global DEM for Greenland (especially concerning thickness of the ice sheet and fjords depth) preclude us to use higher resolution. The local tests (Figure 10) nevertheless show that estimates of eroded masses and thus erosional uplift are conservative, due to the resolution of the data.

In our numerical experiments we consider only the influence of ice load and erosion caused by ice. Even though we demonstrated that these mechanisms play a significant role in land forming processes along Greenland margins, there are other mechanisms that may contribute. One of that processes is a significant thickness of 55 Ma mafic intrusions recorded in the locations considered in our study (e.g., Henriksen, 2008; Figure 2b). Intrusions of 5-10% into several km thick marine sediments may result in uplift counted in hundreds of meters. The concentration of intrusions corresponds roughly to the areas of sediments remaining above sea-level on Figure 9c.

The results of our calculations (Figures 6 and 7) show that northern Greenland has a potentially high influence of the glacial erosion on the landscape forming. That part of Greenland, however, experienced collision with North America (Ellesmere island, west) and Eurasia (Svalbard, east) in the latest Mesozoic to Early Cenozoic when Greenland moves northward (Tessensohn and Piepjohn, 2000). Thus, the landscape of that non-passive margin of Greenland has subjected to active deformation and analysis presented in our study, based solely on the erosion process, may be misleading.

The other part of Greenland margin which represents enigmatic uplift is the area south of Scoresby Sund (Kangerdlugssuaq region, Figure 9). Whereas the geology of Scoresby Sound and northwards is dominated by widespread sedimentary rocks covered by a thin layer of basalt, the area south of the fjord only a thin layer of Cretaceous to Paleogene marine sediments covered by a kilometer-thick basalt layer. It is remarkable that these southern marine deposits rest as much as one kilometer higher than the northern deposits (Myers et al., 1988). This is enigmatic, partly because of the considerable load of overlying basalts, which should have loaded the marine deposits even deeper down, but also because the region is little incised, so that erosional uplift only amounts to 0.4 km for the region while the sediments rests at the elevation of up to 2 km (Figure 9 b or c). Clearly an alternative and dominant source of uplift is needed here. These high altitude marine deposits sits directly on the Iceland hot spot track, where Kangerdlugssuaq passed above the present day position of the Iceland plume at 30 Ma (Lawver and Muller, 1994). The age fits roughly the apatite fission track ages of the region (Hansen, 1996), and it thus seems likely that this mid Cenozoic uplift is related hotspot interaction with Greenland lithosphere.

7. Conclusion

We quantified effects of ice-related processes on shaping margins and internal part of Greenland. Those effects include the influence of the load of massive ice sheet on the Greenland topography and influence of significant erosion caused mainly by glacial carving. Our results show:

(1) Whereas the isostatic response to the load of the Greenland ice sheet is significant, more than 800 m in some areas, within the central Greenland, peripheral flexural bulging is an inefficient mechanism in generating topography along Greenland's margins.

(2) Glacial carving may introduce major vertical motions on Greenland margin and be a major contributor to landscape forming. Our study allowed outlining the areas where this mechanism is potentially important.

(3) We demonstrate how regional observations may be explained using the global model of the Greenland evolution and considering the erosion backward in time. In particular, we consider to which degree erosion may contribute to uplift and tilting of the Nuussuaq peninsula (central west Greenland) and how Mesozoic marine sediments can be uplifted in the central east Greenland margin.

(4) Our numerical experiments with different resolution of topographic data show that the estimation of uplift is conservative.

(5) We point out some regions with significant vertical motions that cannot (Kangerdlugssuaq region with Cretaceous marine sediments at ca. 2 km altitude and only 0.4 km erosional uplift) and should not (e.g., northern Greenland, which is subjected to rather recent tectonic deformations) be analyzed within our purely erosional model.

(6) Our model allows considering the mass balancing processes within and around Greenland; however, this type of study requires more data on the off-shore sediment structure around Greenland. The first order observations show that the volume of offshore sediments in the mouth of the Scoresbysund fjord system is largely insufficient to balance the amount of eroded material inland. This could suggest either that the topography of the fjord is older than the removed Cenozoic offshore sediments and may be linked with other Mesozoic basins around the continental shelf, or that a large proportion of sediments were lost by drifting away from the shelf.

Acknowledgments

This work was supported by a Center of Excellence grant from the Norwegian Research Council to PGP. SM acknowledges support from research grant from Det norske oljeselskap.

AS was supported by Vista and research grant from Chevron to EHH. We thank Johan Bonow and Peter Japsen for data regarding Nuussuaq peninsula profile.

References

Amante, C., and Eakins, B. W., 2009, ETOPO1 1 Arc-Minute Global Relief Model: Procedures, Data Sources and Analysis, NOAA Technical Memorandum NESDIS NGDC-24, 19 p.:

Bamber, J. L., Layberry, R. L., and Gogineni, S., 2001, A new ice thickness and bed data set for the Greenland ice sheet 1. Measurement, data reduction, and errors: Journal of Geophysical Research-Atmospheres, v. 106, no. D24, p. 33773-33780.

Becker, J. J., Sandwell, D. T., Smith, W. H. F., Braud, J., Binder, B., Depner, J., Fabre, D., Factor, J., Ingalls, S., Kim, S. H., Ladner, R., Marks, K., Nelson, S., Pharaoh, A., Trimmer, R., Von Rosenberg, J., Wallace, G., and Weatherall, P., 2009, Global Bathymetry and Elevation Data at 30 Arc Seconds Resolution: SRTM30_PLUS: Marine Geodesy, v. 32, no. 4, p. 355-371.

Berger, D., and Jokat, W., 2009, Sediment deposition in the northern basins of the North Atlantic and characteristic variations in shelf sedimentation along the East Greenland margin: Marine and Petroleum Geology, v. 26, no. 8, p. 1321-1337.

Bonow, J. M., Japsen, P., Lidmar-Bergstrom, K., Chalmers, J. A., and Pedersen, A. K., 2006, Cenozoic uplift of Nuussuaq and Disko, West Greenland - elevated erosion surfaces as uplift markers of a passive margin: Geomorphology, v. 80, no. 3-4, p. 325-337.

Bullard, E., Everett, J. E., and Smith, A. G., 1965, Continental Reconstructions .4. Fit of Continents around Atlantic: Philosophical Transactions of the Royal Society of London Series a-Mathematical and Physical Sciences, v. 258, no. 1088, p. 41-&.

Chalmers, J. A., Pulvertaft, T. C. R., Christiansen, F. G., Larsen, H. C., Laursen, K. H., and Ottesen, T. G., 1993, The southern West Greenland continental margin: rifting history, basin development, and petroleum potential: Geological Society, London, Petroleum Geology Conference series, v. 4, p. 915-931.

Chalmers, J. K., 2000, Offshore evidence for Neogene uplift in central West Greenland: Global and Planetary Change, v. 24, no. 3-4, p. 311-318.

Champagnac, J. D., Molnar, P., Anderson, R. S., Sue, C., and Delacou, B., 2007, Quaternary erosion-induced isostatic rebound in the western Alps: Geology, v. 35, no. 3, p. 195-198.

Champagnac, J. D., Schlunegger, F., Norton, K., von Blanckenburg, F., Abbuhl, L. M., and Schwab, M., 2009, Erosion-driven uplift of the modern Central Alps: Tectonophysics, v. 474, no. 1-2, p. 236-249.

Gaina, C., Gernigon, L., and Ball, P., 2009, Palaeocene-Recent plate boundaries in the NE Atlantic and the formation of the Jan Mayen microcontinent: Journal of the Geological Society, v. 166, p. 601-616.

Gilchrist, A. R., and Summerfield, M. A., 1990, Differential Denudation and Flexural Isostasy in Formation of Rifted-Margin Upwarps: Nature, v. 346, no. 6286, p. 739-742.

-, 1991, Denudation, Isostasy and Landscape Evolution: Earth Surface Processes and Landforms, v. 16, no. 6, p. 555-562.

Haller, J., 1971, Geological map of East Greenland, København, C.A. Reitzels Forlag, 13 col. maps 54 x 66 cm. p.:

Hamann, N. E., Whittaker, R. C., and Stemmerik, L., Geological development of the Northeast Greenland Shelf, *in* Proceedings Petroleum Geology: North-West Europe and Global Perspectives. Proceedings of the 6th Petroleum Conference2005, Geological Society, London. Bath. Geological Society Publishing House, p. 887-902.

Hansen, K., 1996, Thermotectonic evolution of a rifted continental margin: fission track evidence from the Kangerlussuaq area, SE Greenland: Terra Nova, v. 8, no. 5, p. 458-469.

Henriksen, N., 2003, Caledonian orogen, East Greenland 70° - 82° N, Geological map 1:1 000 000: GEUS.

Henriksen, N., 2008, Geological history of Greenland : four billion years of earth evolution, København, Geological Survey of Denmark and Greenland, 272 p. p.:

Japsen, P., Bonow, J. M., Green, P. F., Chalmers, J. A., and Lidmar-Bergstrom, K., 2006, Elevated, passive continental margins: Long-term highs or neogene uplifts? New evidence from West Greenland: Earth and Planetary Science Letters, v. 248, no. 1-2, p. 330-339.

Japsen, P., and Chalmers, J. A., 2000, Neogene uplift and tectonics around the North Atlantic: overview: Global and Planetary Change, v. 24, no. 3-4, p. 165-173.

Japsen, P., Green, P. F., Bonow, J. M., Rasmussen, E. S., Chalmers, J. A., and Kjennerud, T., 2010, Episodic uplift and exhumation along North Atlantic passive margins: implications for hydrocarbon prospectivity: Geological Society, London, Petroleum Geology Conference series, v. 7, p. 979-1004.

Lawver, L. A., and Muller, R. D., 1994, Iceland Hotspot Track: Geology, v. 22, no. 4, p. 311-314.

Leever, K. A., Gabrielsen, R. H., Faleide, J. I., and Braathen, A., 2011, A transpressional origin for the West Spitsbergen fold-and-thrust belt: Insight from analog modeling: Tectonics, v. 30.

Medvedev, S., Hartz, E. H., and Podladchikov, Y. Y., 2008, Vertical motions of the fjord regions of central East Greenland: Impact of glacial erosion, deposition, and isostasy: Geology, v. 36, no. 7, p. 539-542.

Molnar, P., and England, P., 1990, Late Cenozoic Uplift of Mountain-Ranges and Global Climate Change - Chicken or Egg: Nature, v. 346, no. 6279, p. 29-34.

Mosar, J., Eide, E. A., Osmundsen, P. T., Sommaruga, A., and Torsvik, T. H., 2002, Greenland - Norway separation: A geodynamic model for the North Atlantic: Norwegian Journal of Geology, v. 82, no. 4, p. 281-298.

Muller, R. D., Sdrolias, M., Gaina, C., and Roest, W. R., 2008, Age, spreading rates, and spreading asymmetry of the world's ocean crust: Geochemistry Geophysics Geosystems, v. 9, p. 100-120.

Myers, J. S., Dawes, P. R., and Nielsen, T. F. D., 1988, Kort nr. 13, Kangerdlugssuaq: GEUS, Denmark.

Oakey, G. N., and Stephenson, R., 2008, Crustal structure of the Innuitian region of Arctic Canada and Greenland from gravity modelling: implications for the Palaeogene Eurekan orogen: Geophysical Journal International, v. 173, no. 3, p. 1039-1063.

Odell, N. E., 1937, The Glaciers and Morphology of the Franz Josef Fjord Region of North-East Greenland: The Geographical Journal v. 90, no. 2, p. 111-125.

Pelletier, J. D., 2004, Estimate of three-dimensional flexural-isostatic response to unloading: Rock uplift due to late Cenozoic glacial erosion in the western United States: Geology, v. 32, no. 2, p. 161-164.

Schmidt-Aursch, M. C., and Jokat, W., 2005, The crustal structure of central East Greenland - II: From the Precambrian shield to the recent mid-oceanic ridges: Geophysical Journal International, v. 160, no. 2, p. 753-760.

Stern, T. A., Baxter, A. K., and Barrett, P. J., 2005, Isostatic rebound due to glacial erosion within the Transantarctic Mountains: Geology, v. 33, no. 3, p. 221-224.

Swift, D. A., Persano, C., Stuart, F. M., Gallagher, K., and Whitham, A., 2008, A reassessment of the role of ice sheet glaciation in the long-term evolution of the East Greenland fjord region: Geomorphology, v. 97, no. 1-2, p. 109-125.

Tessensohn, F., and Piepjohn, K., 2000, Eocene Compressive Deformation in Arctic Canada, North Greenland and Svalbard and Its Plate Tectonic Causes: Polarforschung, v. 68, p. 121-124.

Tsikalas, F., Faleide, J. I., Eldholm, O., and Wilson, J., 2005, Late Mesozoic–Cenozoic structural and stratigraphic correlations between the conjugate mid-Norway and NE Greenland continental margins: Geological Society, London, Petroleum Geology Conference series, v. 6, p. 785-801.

Wilson, J. T., 1966, Did the Atlantic Close and Then Re-Open?: Nature, v. 211, p. 676-681.